AD-A062 591 THIOKOL CORP HUNTSVILLE ALA HUNTSVILLE DIV F/G 21/9.2

STATISTICAL ANALYSIS OF STEADY STATE COMBUSTION OF COMPOSITE SO--ETC(U)

NOV 78 R L GLICK F49620-76-C-0008

UNCLASSIFIED U-78-15 AFOSR-TR-78-1579 NL

1 OF 1

AD
A062591

END
DATE
FILMED
3-79
DDC

AFOSR-TR- 78-1579

LEVEL II

REPORT NO. U-78-15

AD A062591

STATISTICAL ANALYSIS OF STEADY STATE COMBUSTION OF COMPOSITE SOLID PROPELLANTS

DR. R. L. GLICK
THIOKOL CORPORATION
HUNTSVILLE DIVISION
HUNTSVILLE, ALABAMA 35807

NOVEMBER 1978

FINAL REPORT

DEPARTMENT OF THE AIR FORCE
AIR FORCE OFFICE OF SCIENTIFIC RESEARCH
BOLLING AFB, D.C. 20332

78 11 08 052

Contract/Grant # F49620-76-C-0008

CONTENTS

TABLES

FIGURES

ABSTRACT

A general method for extracting particle size dependent information from experimental rate/formulation data was developed from the statistical methodology. This technique was employed to correlate the data bases of Miller. Results showed that, by employing an interaction parameter of 4 that both additive and additive free data could be correlated to standard error of estimate below 10.5%. The effect of steady radiant energy deposition on steady and nonsteady burning was explored. Results showed that if the radiant energy deposited in the reactive zones is negligible (an excellent assumption for low signature propellants) the effect of radiant energy deposition can always be accounted for by substituting the radiation augmented initial temperature, $T_0^* = T_0 + J_\omega/[\rho c u^0]$, for the initial propellant temperature, T_0.

FINAL REPORT

for

STATISTICAL ANALYSIS OF STEADY STATE COMBUSTION OF COMPOSITE SOLID PROPELLANTS

INTRODUCTION

Background

Solid rocket technology is in a process of dynamic development that is driven by current problems. This process is particularly evident in applications of solid rockets to tactical weapons because of recent emphasis on reduced visible exhaust signature. This emphasis has led to elimination of significant amounts of condensed phase material from the products of combustion and the subsequent creation of a number of problems.

- To maintain specific impulse parity (or to minimize degradation) relative to an "equivalent" metallized formulation the total solids content must be increased. This can lead to physical property and processing problems.

- Replacement of metal additive with oxidizer has altered the relationship among rate, formulation, and environmental variables. Since the bulk of empirical knowledge of these relations resides with metallized formulations, propellant formulation problems have arisen.

- Elimination of condensed phase particulates from the products of combustion degrades stability margins (particularly at higher frequencies) because particle damping is "eliminated". As a consequence, combustion instability has become a very significant design factor.

Clearly, it would be (and is) more difficult to design a solid rocket to specified constraints with low signature propellant than with metallized propellant

The design of solid rockets always strives for a near optimum for imposed constraints. The constraints are set by the level of available technology. It is important to note that there are two basic parts to available technology. First, there is that part concerned with the performance limits of available material; for example, the tensile strength of a case material and the theoretical specific impulse of a propellant. Second, there is that part concerned with the way available materials are arranged into the entity we call a solid rocket motor. Recognition of these two factors is important because available information(1) suggests that insofar as propellant energetics are concerned the first path is peaking. Moreover, the achievement of increased performance along this path is complicated by hazards and cost consideration(1). Consequently, as time passes superior performance will become increasingly dependent upon the potential of inert parts and design excellence.

These are not academic topics; cost robs us of resources and, relative to weaponry, performance can mean our life.

Recent design experience* has amply demonstrated that combustion instability is a major factor in solid rocket design. This may seem surprising in view of the technology that has been developed to treat this problem area to date. However, the simple fact is that existing technology has proven to be too cumbersome for low signature systems. This stems largely from the fact that the direction of combustion instability technology was shaped by instability problems in strategic missile systems --that is, in systems with highly metallized formulations, nearly neutral grains**, and small environmental temperature ranges. In these systems instability needs to be considered at only the lower longitudinal mode frequencies (particulate damping suppresses the higher mode frequencies), and at one pressure and one initial temperature. Therefore, the number of combinations for which data are required is small. Taking pressure, initial temperature, and frequency as variables the number of combinations is on the order of 1-3. On the other hand, in a low signature tactical system instability is not limited to the lower frequency modes. Moreover, non-neutral traces are common (boost/sustain), and the environmental temperature range is substantial (-70 to +170°F). Consequently, the number of combinations is on the order of 20-30. In short, the designer of a low signature tactical system is looking at a task that is roughly an order of magnitude more involved than the designer of a strategic system in order to assure the same "surprise free" design. Consequently, design procedures that "work like a champ" with strategic systems can simply be overwhelmed by the computational and data demands of a low signature, tactical system.

*Reference 2 presents a case study of a recent reduced smoke motor development effort.

**A neutral grain is one that produces a nominally level thrust/time history during the motor's action time.

The point here is simply this. As solid rocket technology shifts to follow the dictates of field experience and mission analyses, the demands made of the technology also shifts. Sometimes these shifts require no new technology while at other times they do. The present is one of the times that new technology is important because:

- o good design is imperative for near-optimum performance,
- o instability is a major design problem in low signature systems, and
- o existing design and data-gathering tools are too cumbersome for the funding levels and development schedules of tactical systems.

To clarify the latter point, consider the design process as it is currently practiced. First, non-detailed trade studies are made to establish the general geometric and propellant properties required to meet the design constraints. Second, a sequence of detailed trade studies are made about one or more baseline designs to establish the "optimal" design in that baseline family. Third, a design is selected for prototype development. The detailed studies include (or should include) detailed performance, structural integrity, and linear stability computations. To carry out performance predictions one needs to know how burning rate varies with pressure, initial temperature, and crossflow. To perform linear stability calculations (with existing codes) one needs to know the cavity geometry, the local mass efflux from the burning surface and the pressure and velocity coupled response functions. The response functions depend upon pressure, initial temperature, crossflow, and frequency. Consequently, carrying out the detailed trade studies requires a substantial amount of propellant ballistic data, particularly when it is recognized that twenty or more formulations may be involved in the trade studies.

Assume, for example, that propellant ballistic data are to be obtained at three pressures, initial temperatures, crossflows, and frequencies. With three replications for statistical significance there are 81 data bits involved in defining burning rate. With the variable area T-burner technique[3] employing data at three area ratios there are 729 data bits for pressure coupled response and an additional 243 data bits for velocity coupled response*. This example serves rather graphically to illustrate the magnitude of the non-steady state ballistic data problem relative to that of the steady-state. When one considers further that thirty tests/day is a very good rate for T-burner testing, that the cost of <u>a</u> T-burner test is on the order of $50, and that twenty or more formulations are usually scrutinized in a motor development program, it is easy to see why stability analyses are always based on incomplete data. The cost required for complete ballistic data is too large a fraction of the total program cost!

---

*This example assumes that flow turning and velocity coupling can be unconfounded.

Contrast the above "tactical" example with a "strategic" example where one pressure, initial temperature and three frequencies, crossflows are involved. Then with three replications 9 data bits are required to define rate, 81 data bits are required to define pressure coupled response, and 27 data bits are required to define velocity coupled response. Thus, as noted before, the magnitude of the ballistic characterization problem and hence the cost and time involved is roughly one order less than for the tactical situation. In contrast, the funding level for the strategic motor development effort is roughly an order of magnitude <u>greater</u> than for the tactical. Therefore, the cost required for complete ballistic data is a much more acceptable fraction (down roughly two orders of magnitude) of total program cost*.

Thus, we are led to an interesting conclusion. The current driving force for upgrading solid rocket design techniques stems not from the strategic but from the tactical! This is not particularly surprizing. It is no challenge to design a Mercedes; it is a <u>challenge</u> to design a Ford that is as good as or superior to a Mercedes.

The above shows rather clearly that a major weakness in current solid rocket design technology is adequate characterization of ballistic properties. It is important to note that design studies are basically <u>quantitative</u> trading operations. Therefore, if inaccurate ballistic properties are employed, the trading operation degenerates to the qualitative level. This is adequate for academic exercises; it is inadequate for the design of propulsion systems that will fly**. This problem can be overcome in two rather different ways.

- Develop more effective methods for defining linear stability properties experimentally.

- Develop more effective ways to extrapolate from a limited data base.

In actuality both paths must be pursued because copious amounts of high quality data are required to test the validity of the extrapolation procedures.

---

*The rotating valve burner under development at CSD[4] offers roughly a three fold reduction in the cost of characterizing nonsteady ballistic properties.

**The knowledgeable reader will certainly note that we have and are getting the design job done without new design tools. However, it is not without considerable "cut and try" at the prototype motor level. This is expensive. Moreover, it shifts emphasis away from an optimal solution and toward <u>any</u> solution. This writer believes that the most critical aspect of the design process is the detailed trade studies and that realism in this phase is critical to the outcome.

AFOSR Statistical Combustion Modeling Program

This program has been aimed at steady-state combustion of polydisperse heterogeneous propellants. The general methodology has been to employ a statistical approach to relate the areal mean burning rate of the propellant to the areal mean burning rate of monodisperse pseudo-propellants whose properties are derived from the statistical formulation. The significance of the arrangement is that it is much easier to model propellant with a single geometric parameter than propellant with a distribution of characteristic dimensions. A monodisperse propellant combustion model has been constructed from the BDP model(5) and combined with the aforementioned statistical procedure to yield a steady-state combustion model for polydisperse, AP-hydrocarbon binder composite propellants. The model has been tested against the extensive data bases generated by Miller, et. al. (6). It has been found that the model is capable of quantitative predictions of the effect of formulation variables on both rate and exponent for additive free formulations. However, predictions/correlations of the data bases with additives (aluminum, iron oxide) were generally poor(7). In addition, it should be noted that formulations with a large(coarse diameter)/(fine diameter) ratio generally showed poorer correlation. These defects have generally been attributed to the fact that the various pseudo-propellants interact more strongly than presently accounted for and that additives influence these interactions.

Subsequent theoretical developments have attempted to extend the theory to include erosive burning(8) and pressure(9) and velocity coupled nonsteady burning**. Insufficient data exists at present for definitive comments at this time. However, the outlook is not promising for the nonsteady extensions. A primary reason for this is the current inability to come to grips with the nonsteady temperature field in the condensed phase of a composite propellant without resort to postulates(10).

In the Background section of the INTRODUCTION it was pointed out that a major problem in the solid rocket design process is collection of adequate nonsteady data. Therefore, the question "why pursue steady-state modeling?" arises quite naturally. The answer is that potential exists for "transforming" steady-state data into nonsteady state "data" for those situations where the characteristic time of the unsteady environment is large compared to the characteristic times of the reactive zones of the process***. That is, a transformation should be possible for those frequencies where the

---

*An areal mean is defined as $\bar{f} = \lim_{S_o \to \infty} \oint_{S_o} f dS/S_o$

**Reference 8 presents an excellent summary of these developments.

***See Reference 11 for a lucid exposition of this.

reactive regions behave quasi-steadily and the transient aspects are confined to the nonreactive condensed phase. This transformation already exists for homogeneous propellants[13]. The difficulty is to extend this methodology to a composite propellant. This is, to all appearances, a formidable problem because at any instant of time the burning surface is composed of all states of all pseudo-propellants. Therefore, some sort of multidimensional solution would appear necessary. Unfortunately, this is beyond the capabilities of present computational machinery. However, during the 1976 work a promising new approach was conceived. For steady-state conditions, the statistics governing an areal mean at fixed time are the same as those for a temporal mean* at fixed location (ergodic theorem[12]). Consequently, for small deviations from steady-state, as might occur for linear, nonsteady process, it should be possible to replace an areal mean (as employed in the steady-state modeling) with a temporal mean. This may seem of small consequence but it opens the door to a one-dimensional methodology for computing nonsteady response for composite propellants. Since the areal mean statistics are known for the pseudo-propellants, the probability of finding any pseudo-propellant in a vertical stack of pseudo-propellants (a "Dagwood sandwich") is known. In addition, for each pseudo-propellant the mean quasi-steady behavior of the reactive zone is known from the steady-state calculations. Moreover, the Z-N methodology[13] tells how to carry these over to the nonsteady state. Therefore, by averaging the response of the vertical stack of pseudo-propellants to fluctuating external conditions the temporal mean is achieved. This should be the areal mean response function desired.

Steady-state combustion modeling is crucial to this enterprise. To apply Z-N methodology one needs to know the behavior of the reactive zone in detail. Quite frankly, the steady-state statistical combustion model supplies exactly this information. Therefore, to the frequency limitation mentioned previously, steady and nonsteady state combustion are rather imtimately connected parts of the same phenomena.

Hopefully, the reader feels as enthusiastic as this writer at this point. Unfortunately, there is a fly in the ointment: the theoretical combustion model works only for additive-free formulations at present, whereas rocket motor propellants invariably contain additives. Thus, one might conclude prematurely that the aforementioned strategy is fit solely for academic purposes.

---

*A temporal mean $\bar{f} = \lim_{\Delta t \to \infty} \int_t^{t+\Delta t} f\,dt/\Delta t$

As noted previously, a statistical combustion model consists of two parts: a statistical framework relating pseudo-propellant properties to propellant properties and a combustion model for computing pseudo-propellant properties. The primary difficulty with current combustion models is an inability to come to quantitative grips with additives. To circumvent this difficulty, note that the required pseudo-propellant information must exist within an adequate steady-state data base. Moreover, by treating the propellant data as knowns and the pseudo-propellant properties as unknowns the statistical framework provides a means for computing pseudo-propellant properties from an adequate steady-state data base. This procedure, for restricted conditions, was developed in 1977 and was found to yield quantitative results for additive free formulations and qualitative results for formulations with additives(7).

Figure 1 illustrates the general strategy at the start of the 1978 program. There are two major paths to the goal of generalizing experimental steady-state data so that it can be employed to predict steady and nonsteady properties of propellants in the same formulation family as the data base. The path through the theoretical model requires a substantially smaller data base than that through the statistical framework. This is its major advantage. The final path to nonsteady properties is not operational. The strategy in 1978 was to push development along both paths. However, because of difficulties encountered along the statistical framework path, little was accomplished on the statistical combustion model path.

In addition to these tasks work was undertaken to determine the effect of thermal radiation on nonsteady pressure coupled burning. This is an obvious scaling factor that must be accounted for in the application of response functions measured in burners of small geometric scale to motors with significantly larger geometric scale. In addition to the obvious technical benefits of pinning down these effects there is the attendant benefit of detailed familiarization with the Z-N methodology to be employed in the subsequent attempt to complete the pseudo-propellant properties to nonsteady properties link.

Accomplishments in 1978 are described in the following section.

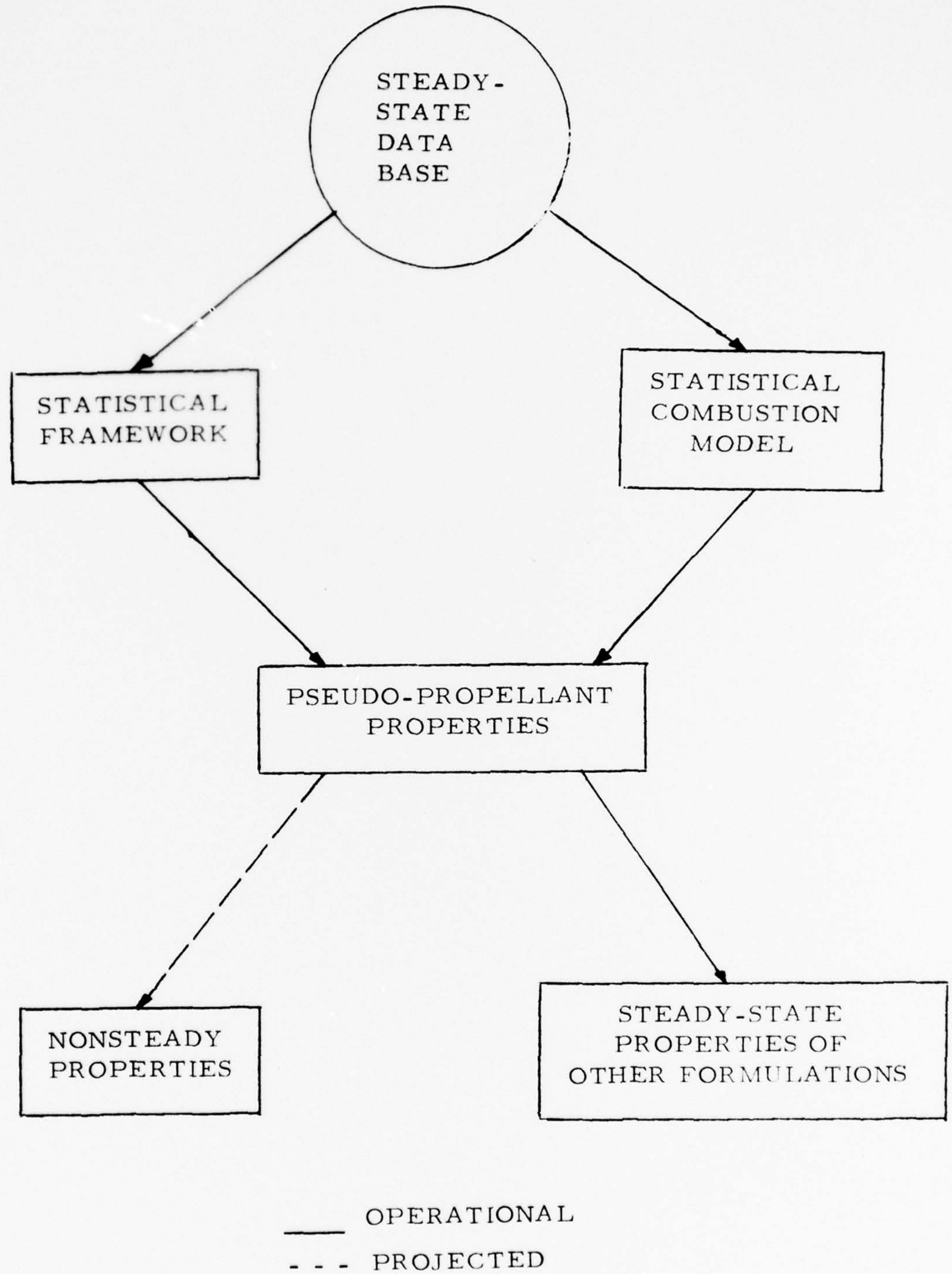

Figure 1. Schematic Illustrating Strategies to Generalize Steady-State Data

ACCOMPLISHMENTS

I. The Effect of Interactions in Statistical Combustion Modeling

The design of solid propellant rockets to maximize "performance" while satisfying envelope, stability, processing, signature, and cost constraints is a complex task. Information central to the successful completion of this task are functional relationships between the steady and nonsteady ballistic parameters needed to predict performance and stability and their independent variables (propellant formulation, pressure, initial propellant temperature, crossflow, frequency). With the large number of independent variables involved experimental definition over the variable ranges involved in many design situations are prohibitively expensive with current techniques. Moreover, the very nature of experimental characterization always leads to discrete rather than continuous information. Since information in discrete form is not generally compatible with optimization strategies, experimental data must first be transformed into a continuous form. Generally speaking, if all other things are equal, a continuous form compatible with physical principles is to be preferred to those devoid of insight because they offer greater potential for accurate interpolation/extrapolation.

In addition to simply correlating experimental data into a continuous form a proper theory also offers potential for an even more desirable goal: transformation of steady-state data into nonsteady state data. This goal is desirable because nonsteady ballistic data are much more expensive to acquire than steady-state data.

In reference 7 a technique was developed that could extract ballistic data in a fundamental form that readily accounted for the effect of particle size on steady-state ballistic properties and held potential for making the steady to nonsteady state transformation possible. Correlations of Miller's additive free data base revealed the ability to accurately correlate rate and exponent data. However, correlation of the additive data showed that the methodology did not, in general, work with propellants containing additives. The objective of this work is to approach this problem again with a more general version of the basic theory.

From statistical combustion theory[14] the mean burning rate of a heterogeneous, propellant with polydisperse oxidizer is related to the burning rate of a sequence of monodisperse pseudo-propellants by

$$\bar{r}_t = \oint_D (\bar{r}^*_{p,d} / \alpha^*_{ox,d}) \, d\omega_d \tag{I-1}$$

where

- o $\bar{r}^*_{p,d}$ is the mean burning rate of the monodisperse pseudo-propellant with oxidizer having $D \leq D \leq D+dD$
- o $\alpha^*_{ox,d}$ is the oxidizer mass fraction of the monodisperse pseudo-propellant with oxidizer having $D \leq D \leq D+dD$, and
- o $d\omega_d$ is the mass fraction of oxidizer with $D \leq D \leq D+dD$.

For most oxidizer grinds it has been shown that a log normal distribution closely approximates the real distribution[15]. Therefore, to a good approximation

$$d\omega_d = \sum_{k=1}^{M} \frac{\alpha_{ox,k}}{\sigma_k \sqrt{2\pi}} \exp\left\{-\left[(\ln D - \ln \bar{D}_k)^2/\sigma_k\right]/2\right\} d \ln D \tag{I-2}$$

It has also been shown[14] that

$$\alpha^*_{ox,d} = \left[1 + 6 C \rho_t D^{m-3} / (\rho_{ox} \pi)\right]^{-1} \tag{I-3}$$

where

$$C = \pi (1 - \zeta_{ox}) / \left(6 \rho_t \oint_D D^{m-3} d\omega_d / \rho_{ox}\right) \tag{I-4}$$

Since $1-\zeta_{ox} = \zeta_b = \rho_t(1-\alpha_{ox})/\rho_b$, Eq. I-4 can be written as

$$\alpha^*_{ox,d} = \left[1 + (1-\alpha_{ox})D^{m-3} \Big/ \oint_D D^{m-3} d\omega_d\right]^{-1} \tag{I-5}$$

Therefore,

$$\bar{r}_t = \oint_D \bar{r}^*_{p,d}\, d\omega_d + \left[(1-\alpha_{ox}) \Big/ \oint_D D^{m-3} d\omega_d\right] \oint_D D^{m-3}\, \bar{r}^*_{p,d}\, d\omega_d \tag{I-6}$$

Variations in the environmental variables do not change the propellant recipe. Therefore, appropriate differentiations of Eq. (I-6) yield

$$\left(\frac{\partial \ln \bar{r}_t}{\partial \ln p}\right)_{T_0} = \bar{n}_t = \oint_D \bar{r}^*_{p,d}\, \bar{n}^*_{p,d}\, d\omega_d + \left[(1-\alpha_{ox}) \Big/ \oint_D D^{m-3} d\omega_d\right] \oint_D D^{m-3}\, \bar{r}^*_{p,d}\, \bar{n}^*_{p,d}\, d\omega_d \tag{I-7a}$$

$$\left(\frac{\partial \ln \bar{r}_t}{\partial T_0}\right)_p = \bar{\sigma}_t = \oint_D \bar{r}^*_{p,d}\, \bar{\sigma}^*_{p,d}\, d\omega_d + \left[(1-\alpha_{ox}) \Big/ \oint_D D^{m-3} d\omega_d\right] \oint_D D^{m-3}\, \bar{r}^*_{p,d}\, \bar{\sigma}^*_{p,d}\, d\omega_d \tag{I-7b}$$

$$\frac{p}{\bar{r}_t}\left(\frac{\partial \bar{r}_t/\partial t}{\partial p/\partial t}\right)_{T_0,v} = \bar{R}_{p,t} = \oint_D \bar{r}^*_{p,d}(\bar{R}^*_p)_d\, d\omega_d + \left[(1-\alpha_{ox}) \Big/ \oint_D D^{m-3} d\omega_d\right] \oint_D D^{m-3}\, \bar{r}^*_{p,d}(\bar{R}^*_p)_d\, d\omega_d \tag{I-7c}$$

$$\frac{\bar{c}}{\bar{r}_t}\left(\frac{\partial \bar{r}_t/\partial t}{\partial v/\partial t}\right)_{T_0,p} = \bar{R}_{v,t} = \oint_D \bar{r}^*_{p,d}(\bar{R}^*_v)_d\, d\omega_d + \left[(1-\alpha_{ox}) \Big/ \oint_D D^{m-3} d\omega_d\right] \oint_D D^{m-3}\, \bar{r}^*_{p,d}(\bar{R}^*_v)_d\, d\omega_d \tag{I-7d}$$

It should be noted that Eqs. (I-6) and (I-7a, b) are, since they arise largely from conservation of mass, and are concerned with means, loosely tied to propellant structure. On the other hand, Eqs. (I-7c, d) are, since time is involved explicitly, more closely tied to propellant structure. If the structure is random, Eqs. (I-7c, d) should hold. If it is ordered, they should not; layer frequency "resonances" would occur.

Equations I-6 - 7d have been employed, with theoretical combustion models to make "a priori" predictions of propellant ballistic properties[7, 9, 15, 17]. Generally, results show excellent correlations for $\bar{r}_t$ and $\bar{n}_t$ with additive free formulations and poor correlations for formulations with additives. Theory/experiment comparisons for $\bar{\sigma}_{p,t}$, $\bar{R}_{p,t}$, and $\bar{R}_{v,t}$ are inhibited by the inadequate data base. In addition, best correlations of theory/experiment occur when m=3 (see Eqs. I-6 and I-7). It is important to note that selection of m=3 is not based on definitive studies; the computational burden is punitive.

Examination of Eq. (I-6) shows that when m=3 it becomes the simple linear relation

$$\bar{r}_t = \sum_{k=1}^{M} \alpha_{ox,k} \bar{r}_k^* / \alpha_{ox} \tag{I-8}$$

where $\alpha_{ox,k}$ is the mass fraction of the kth mode oxidizer in the formulation and $\bar{r}_k^*$ is the burning rate of pseudo-propellant formed from the kth modes oxidizer. With Eq. (I-8) simple linear relations for $\bar{n}_t$, $\bar{\sigma}_{p,t}$ etc that involve the modal pseudo-propellant properties follow easily[7]. Correlations of experimental rate and exponent data have shown that this approach worked extremely well for additive free formulations and some formulations with additives[7]. The question to be asked is "would $m \neq 3$ permit better correlation?" If one attempts to answer this with the theoretical approach, results are confounded with the combustion model's infidelities.

Theoretical computations[15] and experimental reductions[7] both suggest that $r_{p,d}^*$ is a smooth function of ln D. Therefore, it is expected that a "low" order approximation of $\bar{r}_{p,d}^* = f(\ln D)$ over the interval $\ln \bar{D}_1 - 3\sigma_1 \le \ln D \le \ln \bar{D}_M + 3\sigma_M$ would be adequate for the task at hand. The first approach employed a power series approximation.

$$\bar{r}_{p,d}^* = \sum_{i=1}^{M} a_i (\ln D)^i \tag{I-9}$$

for $\bar{r}_{p,d}^*$. The a_i were sought with a nonlinear optimization scheme (PATSH). A major difficulty with this approach became apparent after coding was completed; "optimal" correlations gave $\bar{r}_{p,d}^* < 0$ for some D. Since this is physically impossible, means for "forbidding" these "solutions" are necessary. We could see no simple* way to accomplish this. Consequently, this approach was abandoned in favor of a piecewise linear approach. In this approach the computation process defines $\bar{r}_{p,d}^* = r_i^*$ at specified $\ln D_i$ for i = 1, M. Therefore, extraction of optimal $r_i^* \geq 0$ can be easily guaranteed by employing $r_i^* = |r_i^*|$ in the computational process. This "folds" the $r_i^* < 0$ domain back over the $r_i^* > 0$ domain thereby enabling PATSH to search over both positive and negative r_i^* without an $r_i^* \nless 0$ constraint. Experience has shown that PATSH can become very troublesome when faced

---

*Easy to implement and computationally rapid and effective.

with constraints of this type. Moreover, the extremely valuable feature of the polynomial approach--the ability to evaluate integrals involving D once and for all for each m--is retained. In addition, once an approximation for $\bar{r}^*_{p,d} = f(\ln D)$ has been extracted, the x_i, $i = 1, M$ can be relocated--to provide a better approximation to those regions where $\bar{r}^*_{p,d}$ changes rapidly with ln D.

With the piecewise linear approach ($x = \ln D$)

$$\bar{r}^*_{p,d} = r^*_i + \left[\left(r^*_{i+1} - r^*_i\right)/\left(x_{i+1} - x_i\right)\right]\left(x - x_i\right) \qquad x_i \le x \le x_{i+1} \tag{I-10}$$

Therefore, Eq. I-6 becomes

$$\bar{r}_t = \sum_{i=1}^{M-1}\left[\left(r^*_i - x_i\frac{r^*_{i+1} - r^*_i}{x_{i+1} - x_i}\right)\int_{x_i}^{x_{i+1}} dw_d + \frac{r^*_{i+1} - r^*_i}{x_{i+1} - x_i}\int_{x_i}^{x_{i+1}} x\, dw_d\right] + \frac{1 - \alpha_{ox}}{\oint_D D^{m-3}\, dw_d}\left[\left(r^*_i - x_i\frac{r^*_{i+1} - r^*_i}{x_{i+1} - x_i}\right)\int_{x_i}^{x_{i+1}} D^{m-3}\, dw_d + \frac{r^*_{i+1} - r^*_i}{x_{i+1} - x_i}\int_{x_i}^{x_{i+1}} D^{m-3} x\, dw_d\right] \tag{I-11}$$

With dw_d given by Eq. I-2 this becomes

$$\begin{aligned}\bar{r}_t = \sum_{i=1}^{M-1}\Bigg[&\left(r^*_i - x_i\frac{r^*_{i+1} - r^*_i}{x_{i+1} - x_i}\right)\sum_{k=1}^{M}\frac{\alpha_{ox,k}}{\sigma_k\sqrt{2\pi}}\int_{x_i}^{x_{i+1}}\exp\left[-\frac{1}{2}\left(\frac{x - \bar{x}_k}{\sigma_k}\right)^2\right]dx + \\ &\frac{r^*_{i+1} - r^*_i}{x_{i+1} - x_i}\sum_{k=1}^{M}\frac{\alpha_{ox,k}}{\sigma_k\sqrt{2\pi}}\int_{x_i}^{x_{i+1}} x\exp\left[-\frac{1}{2}\left(\frac{x - \bar{x}_k}{\sigma_k}\right)^2\right]dx + \frac{1 - \alpha_{ox}}{\oint_D D^{m-3}\, dw_d}\left[\left(r^*_i - x_i\frac{r^*_{i+1} - r^*_i}{x_{i+1} - x_i}\right)\sum_{k=1}^{M}\frac{\alpha_{ox,k}}{\sigma_k\sqrt{2\pi}}\int_{x_i}^{x_{i+1}}\exp\Bigg[(m-3)x - \right. \\ &\left. -\frac{1}{2}\left(\frac{x - \bar{x}_k}{\sigma_k}\right)^2\Bigg]dx + \frac{r^*_{i+1} - r^*_i}{x_{i+1} - x_i}\int_{x}^{x_{i+1}} x\exp\left[(m-3)x - \frac{1}{2}\left(\frac{x - \bar{x}_k}{\sigma_k}\right)^2\right]dx\end{aligned} \tag{I-12}$$

Examination of Eq. I-12 shows that there are four types of integrals to be evaluated

$$I^{(1)}_{i,k} = \frac{1}{\sigma_k\sqrt{2\pi}}\int_{x_i}^{x_{i+1}}\exp\left[-\frac{1}{2}\left(\frac{x - \bar{x}_k}{\sigma_k}\right)^2\right]dx \tag{I-13}$$

$$I^{(2)}_{i,k} = \frac{1}{\sigma_k\sqrt{2\pi}}\int_{x_i}^{x_{i+1}} x\exp\left[-\frac{1}{2}\left(\frac{x - \bar{x}_k}{\sigma_k}\right)^2\right]dx \tag{I-14}$$

$$I^{(3)}_{i,k} = \frac{1}{\sigma_k\sqrt{2\pi}}\int_{x_i}^{x_{i+1}}\exp\left[(m-3)x - \frac{1}{2}\left(\frac{x - \bar{x}_k}{\sigma_k}\right)\right]dx \tag{I-15}$$

$$I^{(4)}_{i,k} = \frac{1}{\sigma_k\sqrt{2\pi}}\int_{x_i}^{x_{i+1}} x\exp\left[(m-3)x - \frac{1}{2}\left(\frac{x - \bar{x}_k}{\sigma_k}\right)\right]dx \tag{I-16}$$

Let $u = \frac{x - \bar{x}_k}{\sigma_k \sqrt{2}}$ then $\sqrt{2}\,\sigma_k\, du = dx$ and

$$I^{(1)}_{i,k} = \frac{1}{\sqrt{\pi}} \int_{u_i}^{u_{i+1}} e^{-u^2} du \tag{I-17}$$

The error function is

$$\mathrm{erf}(u) = \frac{2}{\sqrt{\pi}} \int_0^u e^{-y^2} dy \tag{I-18}$$

Thus,

$$I^{(1)}_{i,k} = \frac{1}{2} \left[\mathrm{erf}(u_{i+1} - \mathrm{erf}(u_i) \right] \tag{I-19}$$

Rewrite Eq. I-14 as

$$I^{(2)}_{i,k} = \frac{1}{\sigma_k \sqrt{2\pi}} \left\{ \int_{x_i}^{x_{i+1}} (x - \bar{x}_k) \exp\left[-\frac{1}{2} \left(\frac{x - \bar{x}_k}{\sigma_k} \right)^2 \right] dx + \bar{x}_k \int_{x_i}^{x_{i+1}} \exp\left[-\frac{1}{2} \left(\frac{x - \bar{x}_k}{\sigma_k} \right)^2 \right] dx \right. \tag{I-20}$$

With the above change of variable this becomes

$$I^{(2)}_{i,k} = \bar{x}_k I^{(1)}_{i,k} + \frac{\sigma_k}{\sqrt{2\pi}} \left(e^{-u_i^2} - e^{-u_{i+1}^2} \right) \tag{I-21}$$

Rewrite Eq. I-16 as

$$I^{(4)}_{i,k} = \frac{1}{\sigma_k \sqrt{2\pi}} \int_{x_i}^{x_{i+1}} (x - \bar{x}_k) \exp\left[(m-3)x - \frac{1}{2} \left(\frac{x - \bar{x}_k}{\sigma_k} \right)^2 \right] dx + \frac{\bar{x}_k}{\sigma_k \sqrt{2\pi}} \int_{x_i}^{x_{i+1}} \exp\left[(m-3)x - \frac{1}{2} \left(\frac{x - \bar{x}_k}{\sigma_k} \right)^2 \right] dx \tag{I-22}$$

The latter is recognized as $\bar{x}_k I^{(3)}_{i,k}$. To integrate the former let $w = \exp[(m-3)x]/\sqrt{\pi}$ and $dv = \frac{x - \bar{x}_k}{\sigma_k \sqrt{2}} \exp\left[-\frac{1}{2} \left(\frac{x - \bar{x}_k}{\sigma_k} \right)^2 \right] dx$.

Then

$$v = -\sigma_k\, e^{-\frac{1}{2}\left(\frac{x - \bar{x}_k}{\sigma_k} \right)} / \sqrt{2} \tag{I-23}$$

Consequently

$$\frac{1}{\sigma_k\sqrt{2\pi}}\int_{x_i}^{x_{i+1}}(x-\bar{x}_k)\exp\left[(m-3)x-\frac{1}{2}\left(\frac{x-\bar{x}_k}{\sigma_k}\right)^2\right]dx = \frac{\sigma_k}{\sqrt{2\pi}}\exp\left[(m-3)x-\frac{1}{2}\left(\frac{x-\bar{x}_k}{\sigma_k}\right)^2\right]\Bigg|_{x_{i+1}}^{x_i} + \frac{\sigma_k(m-3)}{\sqrt{2\pi}}\int_{x_i}^{x_{i+1}}\exp\left[(m-3)x-\frac{1}{2}\left(\frac{x-\bar{x}_k}{\sigma_k}\right)^2\right]dx \tag{I-24}$$

Thus,

$$I_{i,k}^{(4)} = \left[\bar{x}_k+(m-3)\sigma_k^2\right]I_{i,k}^{(3)} - \frac{\sigma_k}{\sqrt{2\pi}}\exp\left[(m-3)x-\frac{1}{2}\left(\frac{x-\bar{x}_k}{\sigma_k}\right)^2\right]\Bigg|_{x_i}^{x_{i+1}} \tag{I-25}$$

With Eqs. I-2 and I-15

$$\oint_D D^{m-3}\,dw_q = \sum_{i=1}^{M-1}\sum_{k=1}^{M}\alpha_{ox,k}I_{i,k}^{(3)} = \sum_{k=1}^{M}\alpha_{ox,k}\sum_{i=1}^{M-1}I_{i,k}^{(3)} = \sum_{k=1}^{M}\alpha_{ox,k}I_k^{(3)} \tag{I-26}$$

Attempts to reduce the remaining integrals to defined functions fail because integrals involving the integral of the error function appear. Consequently, $I_{i,k}^{(3)}$ is evaluated by numerical quadrature.

With these terms Eq. I-12 can be rewritten as

$$\begin{aligned}\bar{r}_t = \sum_{i=1}^{M-1}\Bigg\{&\left(r_i^*-x_i\frac{r_{i+1}^*-r_i^*}{x_{i+1}-x_i}\right)\sum_{k=1}^{M}\alpha_{ox,k}\left(I_{i,k}^{(1)}+\frac{1-\alpha_{ox}}{\sum_{i=1}^{M-1}\alpha_{ox}\sum_{k=1}^{M}I_{i,k}^{(3)}}I_{i,k}^{(3)}\right)+\\&+\frac{r_{i+1}^*-r_i^*}{x_{i+1}-x_i}\sum_{k=1}^{M}\alpha_{ox,k}\left[\bar{x}_k I_{i,k}^{(1)}+\frac{\sigma_k}{\sqrt{2\pi}}\left(e^{-u_i^2}-e^{-u_{i+1}^2}\right)+\frac{1-\alpha_{ox}}{\sum_{k=1}^{M}\alpha_{ox,k}\sum_{i=1}^{M-1}I_{i,k}^{(3)}}I_{i,k}^{(3)}\right]\Bigg\}\end{aligned} \tag{I-27}$$

For each of Miller's formulation series[6] α_{ox}, $\bar{x}_k$, σ_k are fixed. Therefore, $I_{i,k}^{(1)}$ can be evaluated once and for all and $I_{i,k}^{(3)}$ can be computed once for each m.

Equation I-27 gives $\bar{r}_t$ in terms of the r_i^*. To evaluate the r_i a nonlinear optimizer (PATSH) and Miller's data base were employed. Basically, a subset of Miller's data base was input, m was specified, and the optimizer selected the r_i^* such that the standard error of estimate between prediction and data was minimized. Appendix B tabulates the FORTRAN IV code that was employed.

Table I-1 presents the standard error of estimates achieved. The most striking feature of these results is that the correlation improves as m increases. On theoretical grounds one would expect to see $m \sim 2$; on the basis of limited model computations it was found that $m \sim 3$ effected better correlation than $m \sim 2$ (no computations with $m > 3$ were made); these results show that best correlation is achieved with $m \sim 4$. Note that with $m = 4$ that <u>all</u> of Miller's rate data is correlated with standard error of estimates below 10.5%.

TABLE I-1

CORRELATION RESULTS

DATA SET	PRESSURE psi	m	SEE,* %	COMMENTS
SD-I-88	500	2.0	6.34	88% total solids,
	1000	2.0	12.65	18% 24μ Al.
	2000	2.0	20.36	
	1000	0.5	14.54	
	1000	1.0	14.29	
	1000	1.5	13.97	
	1000	2.5	11.38	
	1000	3.0	8.13	
	1000	4.0	5.48	
SD-III-88	500	2.0	4.31	88% total solids,
	1000	2.0	6.65	no additives
	2000	2.0	11.25	
	500	3.0	3.05	
	1000	3.0	4.49	
	2000	3.0	7.57	
	500	4.0	2.6	
	500	4.5	2.16	
SD-IV-88	500	4.0	4.03	88% total solids,
	1000	4.0	6.54	18% 90μ Al.
	2000	4.0	10.49	
SD-V-88	500	4.0	1.68	88% total solids,
	1000	4.0	2.36	18% 6μ Al.
	2000	4.0	4.52	
SD-VI-90	500	4.0	1.08	90% total solids,
	1000	4.0	2.53	21% 24μ Al.
	2000	4.0	5.52	
SD-VII-88	500	4.0	1.39	88% total solids,
	1000	4.0	3.62	18% 24μ Al.
	2000	4.0	3.91	+ 1% Fe_2O_3

*Standard Error of Estimate

Examination of the results for the SD-I and SD-III series suggests that correlation is not strongly dependent upon m for the additive free formulations. However, for formulations with additives use of $m \sim 4$ substantially improves the correlation . It is interesting to note that in every case the correlation degrades as pressure increases.

Figures I-1, I-2, and I-3 present the computed pseudo-propellant rates as a function of oxidizer particle size. For $m \sim 3$[7] these rates tended toward an asymptotic limit as diameter approached zero and to zero as diameter increased. These results for $m = 4$ show a much more complex multi-extremum behavior. For the formulations with aluminum as the sole additive burning rate decreases toward zero with decreasing diameter for diameters below $1\,\mu$. However, with the addition of 1% Fe_2O_3 this trend is reversed and burning rate increases with decreasing diameter for diameters below $1\,\mu$.

These calculations have shown that by employing $m \sim 4$ that rate/particle size data can be correlated and diameter dependent pseudo-propellant properties extracted for formulations with and without additives. If this technique remains valid for temperature sensitivity data (insufficient data currently exists to say either yea or nay), the pseudo-propellant properties needed for a composite propellant Z-N model can be extracted.

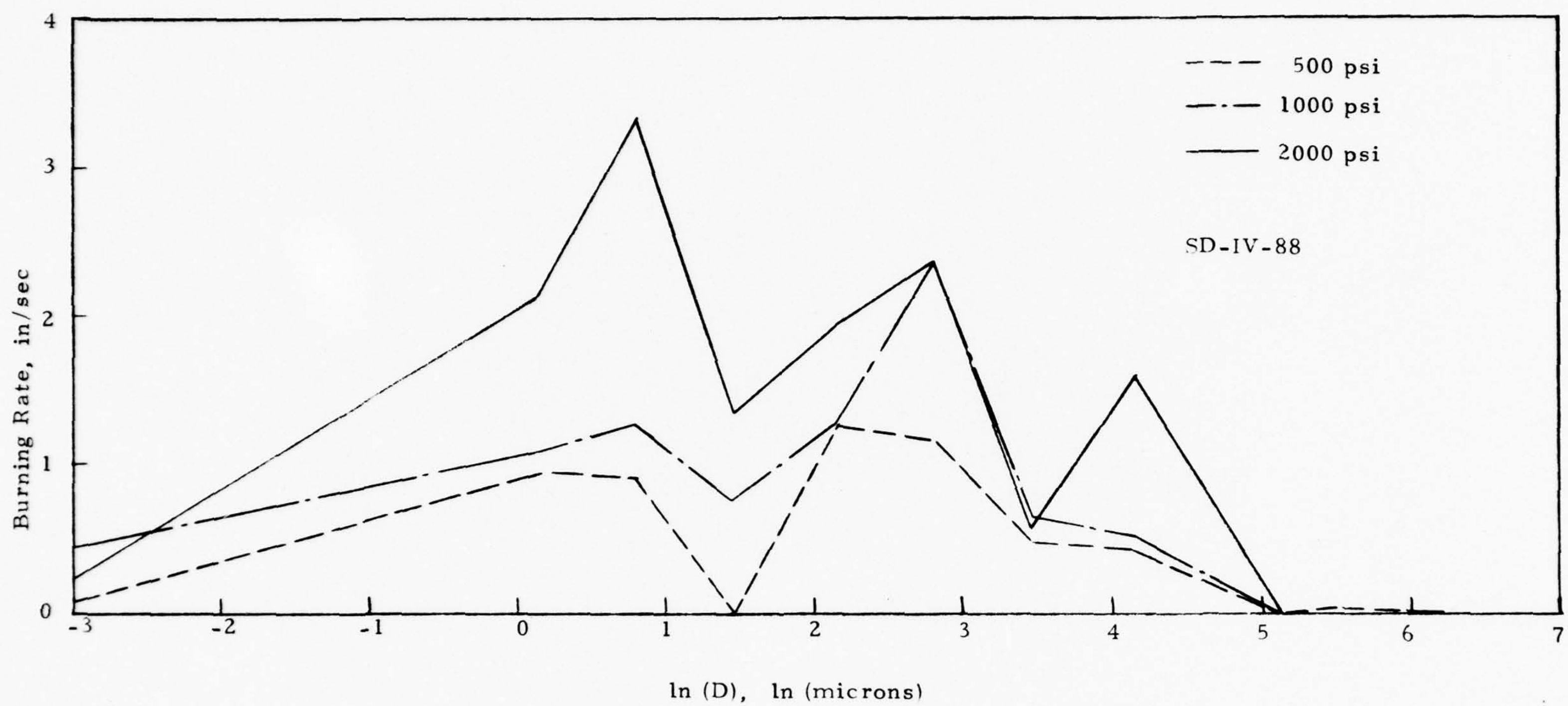

Figure I-1. Pseudo-Propellant Burning Rates For Miller's SD-IV-88 Formulation Series When $m = 4.0$

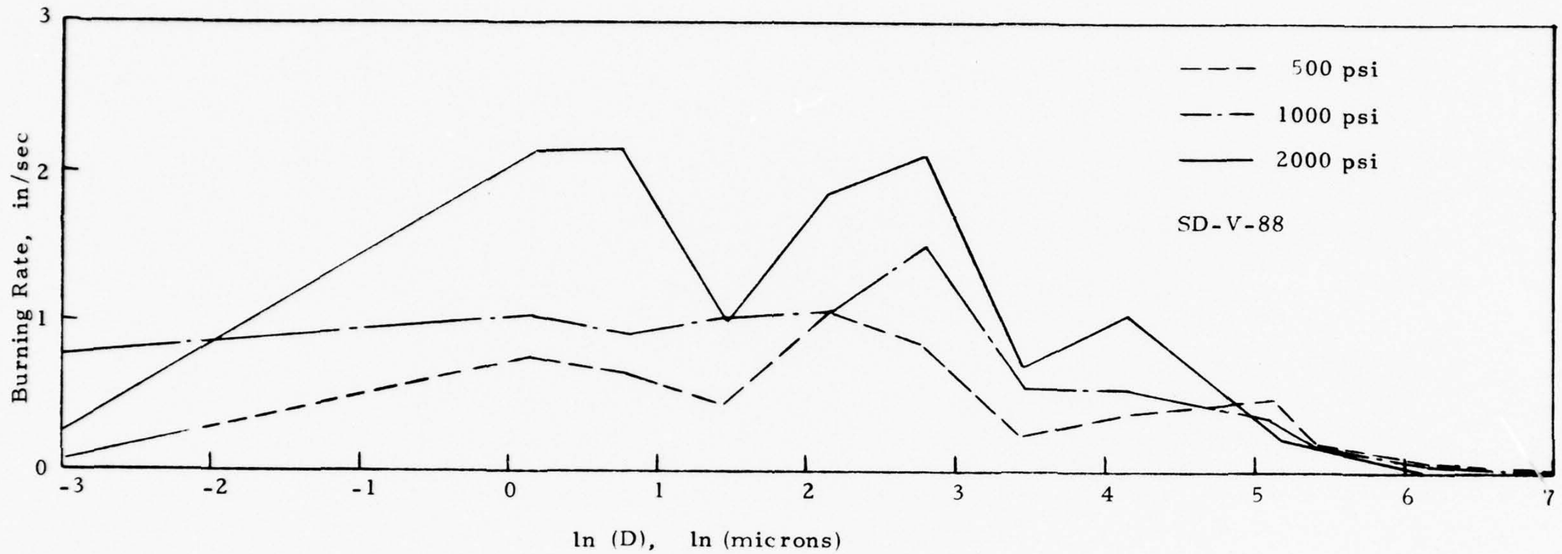

Figure I-2. Pseudo-Propellant Burning Rates for Miller's SD-V-88 Formulation Series When m = 4.0

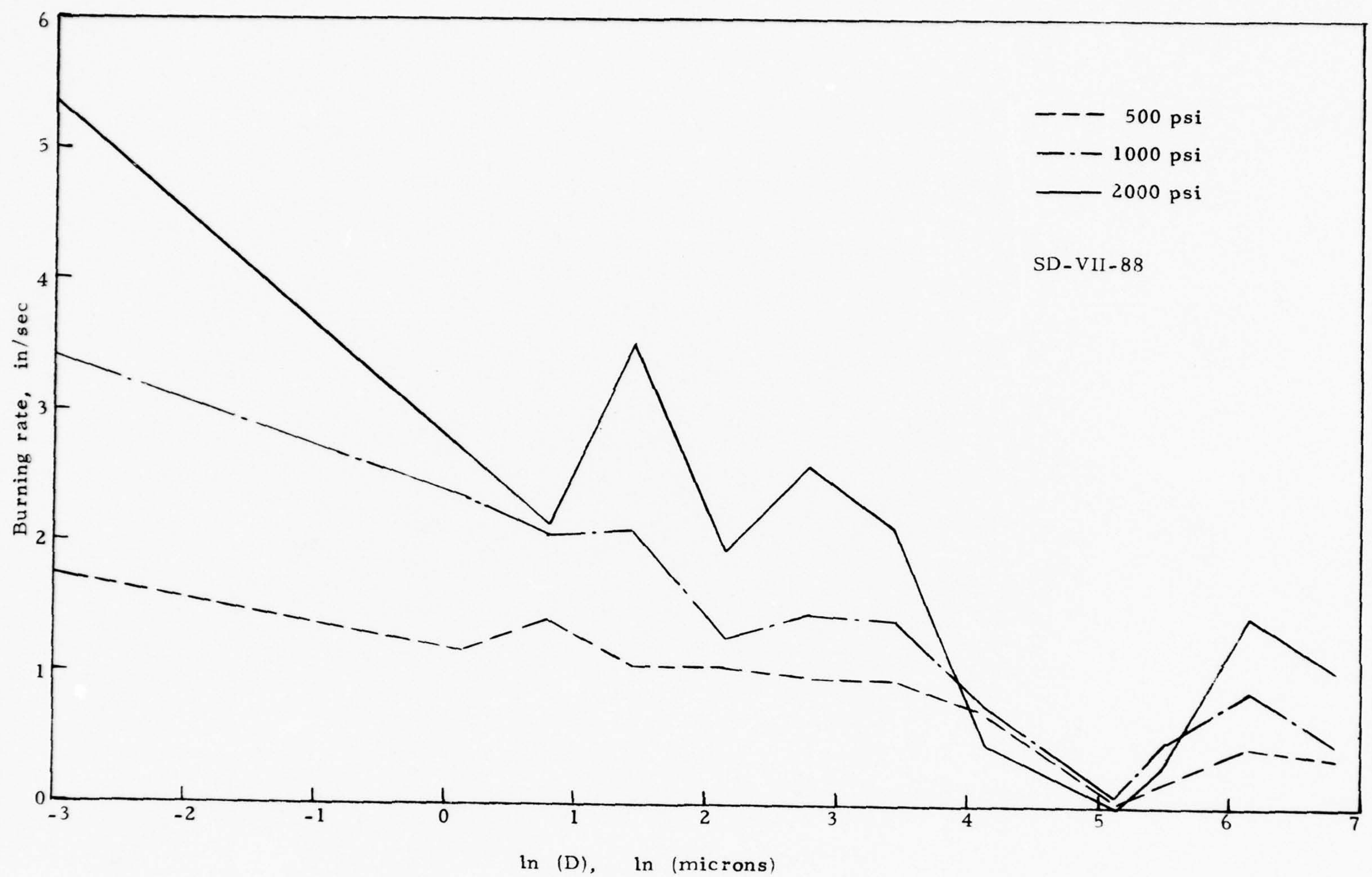

Figure I-3. Pseudo-Propellant Burning Rates for Miller's SD-VII-88 Formulation Series When $m = 4.0$

II. The Effect of Thermal Radiation on Pressure Coupled Response

Methodology for computing the linear stability margin of a solid propellant rocket motor includes testing propellant in a small scale laboratory burner (T-burner, SEV-burner, rotating valve burner) to determine its response to pressure and crossflow oscillations. These response functions are then employed in linear stability calculations for full scale motors. For this process to be useful the response function in the motor environment must be either that of the laboratory burner or scalable from it. At present, little is known about this scaling process because neither response functions nor motor stability margins can be defined with precision. Calculations have demonstrated that the time mean flow field in a rocket motor is dependent upon its geometric scale[16] and that crossflow can effect pressure and velocity coupled response in "strange" ways[17]. Therefore, potential exists for significant scaling effects. However, even in the situation of pressure coupling without crossflow there is still an environmental difference between burner and motor. In the motor radiosity at the burning surface will be larger than in the burner because the beam length is larger and the "walls" are hotter. This will be particularly true for reduced and minimum smoke propellants because their effective gas emissivities will be less than those of propellants whose products contain significant amounts of condensed phase particulates.

It is known that radiosity level can alter burning rate. In most cases this effect is small ($<10\%$). Therefore, on these grounds one might dismiss the effect. However, radiation, since it deposits energy in the condensed phase, directly alters the subsurface thermal field. This may alter the frequency dependent character of the response functions. Two extreme situations appear to exist. If the extinction depth of the radiation is much larger than the thermal wave thickness ($\ell_R \gg \varkappa/u^\circ$), the majority of the energy deposition will occur beyond the thermal wave, the important characteristic length is still the thermal wave thickness, and the propellant will appear to be preheated. For a specific "homogeneous" propellant[18]

$$R_p \sim R_p(\varkappa\omega/[u^\circ]^2)$$

Therefore, for this situation the effect of radiosity would be to alter the response function by

$$\delta R_p \sim -2[\varkappa\omega/(u^\circ)^2]\, R_p'\, \sigma_p\, \delta T_0$$

where $\delta T_0 \sim \frac{J_a}{\rho u^\circ c}$. However, if the extinction depth is smaller than the thermal wave thickness ($\ell_R < \varkappa/u^\circ$), the majority of the energy deposition will occur within the thermal wave; there will be two characteristic thermal lengths (ℓ_R and $\varkappa/u^\circ$); and possibility for "resonance amplification" exists.

If propellant is homogeneous, radiant energy will be deposited in exponential fashion and penetration will depend solely upon the extinction length of the propellant. However, if the propellant is heterogeneous, radiant energy deposition will depend upon both the constituents transmissivities and the propellant's structure. The problem of radiant transfer in a heterogeneous media is difficult. The purpose here is not to solve this problem. Rather, the intent is to examine qualitative aspects of the effects of radiation on pressure coupled response. Toward this end two limiting cases will be examined. In the first the propellant is considered homogeneous for both radiant energy deposition and conductive transport. In the second, the propellant is considered to be black, opaque binder and transparent oxidizer for radiant energy deposition and homogeneous for conductive transport. These represent simplistic models for homogeneous and heterogeneous propellants.

The path to a solution of this problem will be to define radiant energy deposition in both cases. For the heterogeneous propellant model statistical combustion modeling results[14] will be employed. The effect of this radiant energy deposition on pressure coupled response will be determined by employing Z-N methodology[13]. This is founded upon the following basic assumptions.

- The propellant is homogeneous.
- The reactive zones behave quasi-steadily.
- Functions $u^\circ(p^\circ, T_o)$ and $T_s^\circ(p^\circ, T_o)$ are defined by experimental data.

The first assumption is common to all existing "exact" analyses of nonsteady combustion. The second implies both an upper bound on frequency for validity and that condensed phase reactions are constrained to the surface. Relative to the latter assumption it is important to note that only partial derivatives of these functions appear explicitly. Therefore, these data must be very accurate. Since T_s° data are virtually unobtainable (for heterogeneous propellants the concept of <u>a</u> surface temperature is incorrect and anything but accurate and u° data are not very precise, Z-N methodology is currently inoperable in its originators context. Consequently, "why pursue the Z-N approach?" There are four parts to the answer. First, the Z-N method does not imply any reactive zone model. Therefore, it can employ all. Second, a path to predicting the nonsteady response of heterogeneous propellants has been devised that employs Z-N concepts[13]. Third, better methods are being devised to measure $u^\circ(p^\circ, T_o)$. Fourth, the possibility of replacing T_s° data with more readily obtainable nonsteady data exists. Therefore, future promise justifies use of the Z-N method.

For homogeneous propellant*

$$dJ = J\,dx/\ell_R \tag{II-1}$$

Integration and application of the boundary condition

$$J(o) = J_s \tag{II-2}$$

gives

$$J = J_s\, e^{x/\ell_R} \tag{II-3}$$

The radiant energy deposition per unit volume is, from a radiant energy balance,

$$\Phi = dJ/dx \tag{II-4}$$

With (II-3) this becomes

$$\Phi = J_s\, \ell_R^{-1}\, e^{x/\ell_R} \tag{II-5}$$

Thus, for homogeneous propellant energy is deposited in exponential fashion. Note that unsteadiness in Φ is associated with unsteadiness in J_s.

If the propellant is heterogeneous with black, opaque binder and transparent oxidizer, radiant energy will be deposited at the binder surface and at oxidizer binder interfaces beneath that surface. With this simplistic model radiant energy deposition will depend solely upon the oxidizer particle size distribution.

Consider the single oxidizer particle illustrated by Figure II-1. Radiant energy enters the exposed, convex surface (a, b). It is assumed that this surface is "rough" so that it appears to be a diffuse emitter. Therefore, the radiant energy crossing S(o) is also the energy entering the subsurface. Since S(o) cannot see itself

$$F_{S(o)\to S(x)} + F_{S(o)\to S_3} = 1 \tag{II-6}$$

and

$$F_{S(o)\to S(x+dx)} + F_{S(o)\to S_3} + dF_{S(o)\to dS_3} = 1 \tag{II-7}$$

Combining (II-6) and (II-7) yields

$$dF_{S(o)\to dS_3} = -(\partial F_{S(o)\to S(x)}/\partial x)\,dx \tag{II-8}$$

---

*Since $O(T_{FLAME}) > O(T_{PROP})$, $O(J_{f\to p}) \sim 10^4\, O(J_{p\to f})$. Therefore, $J_{f\rightleftarrows p} \sim J_{f\to p} \sim J$.

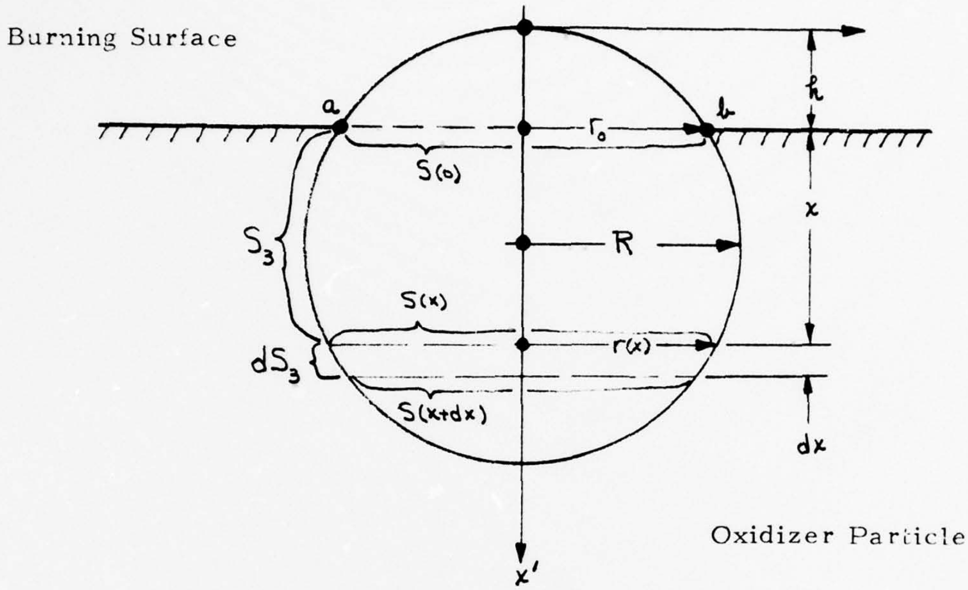

Figure II-1. View Factor Geometry

For opposed, parallel disks like S(o) and S(x) Sparrow and Cess[19] give

$$F_{S(o)\to S(x)} = \left[(r_o^2 + r_x^2 + x^2) - \sqrt{(r_o^2 + r_x^2 + x^2) - 4r_o^2 r_x^2}\,\right] / (2r_o^2) \tag{II-9}$$

If the terms in (II-9) are non-dimensionalized with the particle diameter D, the form of the equation does not change. Therefore, (II-9) can be employed in nondimensional form (denoted by an overbar). For a circle with center at $(r, x^l) = (O, R)$

$$r^2 + (x' - R)^2 = R^2 \tag{II-10}$$

Thus,

$$\bar{r} = \bar{x}'(1 - \bar{x}') \tag{II-11}$$

so that

$$\bar{r}_o^{\,2} = \bar{h}(1 - \bar{h}) \tag{II-12}$$

and

$$\bar{r}_x^{\,2} = (\bar{h} + \bar{x})(1 - \bar{x} - \bar{h}) \tag{II-13}$$

Substitution of (II-12) and (II-13) into (II-9) yields (with difficulty)

$$F_{S(o)\to S(x)} = 1 + \bar{x}/(1 - \bar{h}) \qquad (0 \le \bar{h} < 1 \,;\; 0 \le \bar{x} < 1 - \bar{h}) \tag{II-14}$$

Therefore, with (II-8)

$$dF_{S(o)\to dS_s} = -(1 - \bar{h})^{-1} d\bar{x} \tag{II-15}$$

The number of oxidizer particles on the burning surface S_p with h and D is[14]

$$d^2N = [6/(\pi D^3)]\, S_p \, dJ_d \, dh \tag{II-16}$$

Since the area of the intersection of one of these particles with S_p is

$$S(o) = \pi r^2 = \pi h (D - h) \tag{II-17}$$

the planar surface area of these particles at the burning surface (x=o) is

$$d^2 S_o = 6\bar{h}(1 - \bar{h})\, S_p \, dJ_d \, d\bar{h} \tag{II-18}$$

Therefore, the radiant energy entering these particles is

$$d^3\mathcal{J} = 6 J_s \bar{h}(1-\bar{h})\, S_p\, d\zeta_d\, d\bar{h} \tag{II-19}$$

The fraction of this energy deposited at $(h-D) \le x \le 0$ is

$$d^3\mathcal{J} = dF_{S(\theta)\to dS_3}\, d^2\mathcal{J} \tag{II-20}$$

With I-15, I-19, and I-20

$$d^3\mathcal{J} = 6 J_s \bar{h}\, S_p\, d\zeta_d\, d\bar{h}\, dx/D \tag{II-21}$$

Since $J = \mathcal{J}/S_p$ and $\Phi = dJ/dx$

$$d^2\Phi = 3D^{-1} J_s\, d\zeta_d\, d\bar{h}^2 \tag{II-22}$$

To deposit energy at depth $-1 < \bar{x} \le 0$, $0 < \bar{h} < (1+\bar{x})$. Therefore, the energy deposited at x by all oxidizer particles with diameter D is

$$d\Phi = 3D^{-1} J_s\, d\zeta_d \int_0^{(1+\bar{x})^2} d\bar{h}^2 \tag{II-23}$$

Consequently,

$$\begin{aligned} d\Phi &= 3D^{-1} J_s (1+x/D)^2\, d\zeta_d & -D \le x \le 0 \\ &= 0 & x < -D \end{aligned} \tag{II-24}$$

It has been demonstrated elsewhere[15] that the particle size distribution in an oxidizer mode is nearly log normal. Therefore[14],

$$d\zeta_d = \frac{\rho_{ox}}{\rho_*} \sum_{k=1}^{M} \frac{\alpha_{ox,k}}{\sigma_k \sqrt{2\pi}} \exp\left[-\frac{1}{2}\left(\frac{\ln D - \ln \bar{D}_k}{\sigma_k}\right)^2\right] d\ln D \tag{II-25}$$

Since only those particles with $D \ge |x|$ can deposite energy at x

$$\Phi = 3 J_s \frac{\rho_{ox}}{\rho_*} \sum_{k=1}^{M} \frac{\alpha_{ox,k}}{\sigma_k\sqrt{2\pi}} \int_{\ln|x|}^{\infty} D^{-1}(1+x/D)^2 \exp\left[-\frac{1}{2}\left(\frac{\ln D - \ln\bar{D}_k}{\sigma_k}\right)^2\right] d\ln D \tag{II-26}$$

Note that unsteadiness in Φ *is associated with that of* J_s.

Figure 2 sketches the general phenomena involved in the combustion process. The process is divided into two major parts: the nonreactive condensed phase $(x < o)$ and the reactive region $(x > o)$. The latter is depicted as containing two subregions--a gas phase reaction zone and a condensed phase reaction zone. As demonstrated by Novozhilov[13] and Summerfield, et. al.[11], the characteristic time of the reactive zone has lesser order of magnitude than that of the nonreactive condensed phase. Accordingly, when the order of magnitude of the characteristic time of any transient process is greater than that of the reactive zone, the reactive zone will respond in quasi-steady fashion. That is, "inertia" will be confined to the nonreactive condensed phase. The upshot of this is that the reactive region may be described by appropriate steady-state relations.

Moreover, if the radiative extinction length of the gaseous products and the condensed phase is large compared with the gas phase and condensed phase reactive zone thicknesses respectively*, radiation will not interact significantly with the reactive zone. This seems to be a very plausible assumption for reduced and minimum smoke propellants. This means that for a specified formulation the reactive zones mass flux is defined solely by its boundary conditions (T_s, f) and environment (p). In short,

$$m_r^\circ = m_r^\circ(\text{formulation}, T_s, f, p) \tag{II-27}$$

where $(\ )^\circ$ denotes steady-state conditions. If the reactive zone is quasi-steady

$$m_r^\circ(T_s^\circ, f^\circ, p) = m_r(T_s, f, p) \tag{II-28}$$

and

$$\rho u^\circ = m_r^\circ = \rho u \tag{II-29}$$

Thus, for a quasi-steady reactive zone the instantaneous burning rate is, for fixed formulation, functionally related as

$$u = m_r^\circ(T_s, f, p)/\rho \tag{II-30}$$

Note that if radiation does not interact with the reactive zone that this relation holds irregardless of the radiant flux level.

*If the extinction length is small compared to these dimensions, the geometric scale of the motor's cavity will not significantly influence the radiant flux incident on the reactive zone, and the incident radiative flux becomes another independent variable for m_g. Reference 20 has attacked this problem.

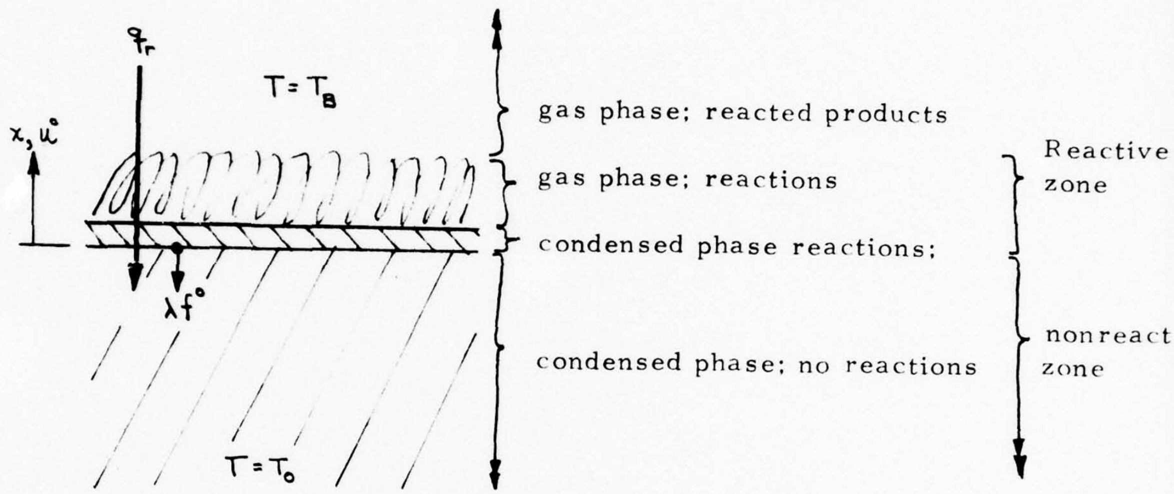

Figure II-2. Sketch of Regions in Combustion Process

In principle, one may obtain both $u^\circ(p, T_0)$ and $T_{s0}^\circ(p, T_0)$ from steady-state experiments. In the absence of radiation an energy balance (steady-state) for the x = 0 to x = ∞ region yields

$$\kappa f_0^\circ = u_0^\circ (T_{s0}^\circ - T_0) \tag{II-31}$$

With $T_{s0}^\circ(p, T_0)$ known, Eq. (II-31) gives $T_0(p, f_0^\circ)$. Therefore, $u_0^\circ(p, T_0)$ and $T_{s0}^\circ(p, T_0)$ can be rewritten as

$$u_0^\circ = u_0^\circ(p, f_0^\circ) \; , \; T_{s0}^\circ = T_{s0}^\circ(p, f_0^\circ) \tag{II-32}$$

Clearly, if p, f_0° are specified, T_{s0}° is also defined and u_0° is determinable from Eq. (II-30); that is, from the reactive zone solution. Therefore, Eq. (II-32) is quasi-steady.

Under the "optical thin assumption", the reactive zone is independent of radiation. Therefore, the connections must become

$$u_0^\circ(p, f_0^\circ) = u^\circ(p, f^\circ) \; , \; T_{s0}^\circ(p, f_0^\circ) = T_s^\circ(p, f^\circ) \tag{II-33}$$

Finally since Eq. (II-30) holds

$$u_0^\circ(p, f_0^\circ) = u(p, f) \, , \; T_{s0}^\circ(p, f_0^\circ) = T_s(p, f) \tag{II-34}$$

If there is radiation, the energy balance (steady-state) becomes

$$\kappa f^\circ = u^\circ [T_s^\circ - (T_0 + J/\rho c u^\circ)] \tag{II-35}$$

Therefore, since the connections have been demonstrated to be associated with the reactive zone and that zone is not effected by radiation, it makes no difference whether f_0° or f° is employed. With equivalence of f_0° and f° Eqs. (II-31) and (II-35) show that radiation may be accounted for in *steady-state* by employing the equivalent initial temperature

$$T_0^* = T_0 + J/\rho c u^\circ \tag{II-36}$$

In other words, in the *steady-state* radiant energy deposition and initial temperature change produce equivalent effects and Eq. (II-36) demonstrates the equivalent temperature for specified T_0 and J.

The equation governing the nonsteady thermal field in the non-reactive condensed phase $(x < o)$ is[13]

$$\rho c \frac{\partial T}{\partial t} + \rho c u \frac{\partial T}{\partial x} = \lambda \frac{\partial^2 T}{\partial x^2} + \Phi \tag{II-37}$$

The boundary conditions are

$$T(-\infty, t) = T_o \;, \quad T(o,t) = T_s \tag{II-38}$$

and the connections are

$$u = u(f, p) \;, \quad T_s = T_s(f, p) \tag{II-39}$$

where $f = (\partial T/\partial x)_{x=0}$. Introducing dimensionless variables

$$\begin{aligned} &v = u/u^\circ,\ \xi = u^\circ x/\varkappa,\ \tau = (u^\circ)^2 t/\varkappa,\ \eta = p/p^\circ,\ \psi = \Phi/\Phi^\circ,\ \varphi = f/f^\circ; \\ &\Theta = (T - T_o^*)/(T_s^\circ - T_o^*),\ \vartheta = (T_s - T_o^*)/(T_s^\circ - T_o^*),\ \zeta^\circ = \Phi^\circ(\varkappa/u^\circ)/[\rho c u^\circ (T_s^\circ - T_o^*)] \end{aligned} \tag{II-40}$$

yields

$$\frac{\partial \Theta}{\partial \tau} = \frac{\partial^2 \Theta}{\partial \xi^2} - v \frac{\partial \Theta}{\partial \xi} + \psi \zeta^\circ \tag{II-41}$$

with boundary conditions

$$\Theta(-\infty, \tau) = (T_o - T_o^*)/(T_s^\circ - T_o^*) = -\alpha \;, \quad \Theta(o, \tau) = \vartheta \tag{II-42}$$

and connections

$$v = v(\varphi, \eta) \;, \quad \vartheta = \vartheta(\varphi, \eta) \tag{II-43}$$

Assume that small, periodic pressure and radiation changes are imposed. That is assume

$$\eta = 1 + \hat{\eta}_1 e^{i\gamma\tau} \;, \quad \psi = 1 + \hat{\psi}_1 e^{i\gamma\tau} \tag{II-44}$$

where $O(\hat{\psi}_1) \sim O(\hat{\eta}_1) < 1$. Then, in response to these fluctuations

$$\Theta(\xi,\hat{\tau}) = \Theta^{\circ}(\xi) + \hat{\eta}_1 \Theta_{1\eta}(\xi,\hat{\tau}) + \hat{\psi}_1 \Theta_{1\psi}(\xi,\hat{\tau})$$

$$\upsilon(\hat{\tau}) = 1 + \hat{\eta}_1 \upsilon_{1\eta}(\hat{\tau}) + \hat{\psi}_1 \upsilon_{1\psi}(\hat{\tau}) \qquad \text{(II-45)}$$

Substitution of these functions into Eq. II-41 and neglect of higher order terms yields

$$\hat{\eta}_1\left(\frac{\partial\Theta_{1\eta}}{\partial\hat{\tau}} - \frac{\partial^2\Theta_{1\eta}}{\partial\xi^2} + \frac{\partial\Theta_{1\eta}}{\partial\xi} + \upsilon_{1\eta}\frac{\partial\Theta^{\circ}}{\partial\xi}\right) + \hat{\psi}_1\left(\frac{\partial\Theta_{1\psi}}{\partial\hat{\tau}} - \frac{\partial^2\Theta_{1\psi}}{\partial\xi^2} + \frac{\partial\Theta_{1\psi}}{\partial\xi} + \upsilon_{1\psi}\frac{\partial\Theta^{\circ}}{\partial\xi} - e^{i\lambda\hat{\tau}}\zeta^{\circ}\right) = \frac{d^2\Theta^{\circ}}{d\xi^2} - \frac{d\Theta^{\circ}}{d\xi} + \zeta^{\circ} \qquad \text{(II-46)}$$

Since this equation must hold for $\hat{\eta}_1 = \hat{\psi}_1 = 0$, $\hat{\eta}_1 = 0$ and $\hat{\psi}_1 = 0$

$$\frac{d^2\Theta^{\circ}}{d\xi^2} - \frac{d\Theta^{\circ}}{d\xi} + \zeta^{\circ} = 0 \qquad \text{(II-47)}$$

with boundary condition

$$\Theta^{\circ}(-\infty) = -\alpha \; , \quad \Theta^{\circ}(0) = \vartheta^{\circ} \qquad \text{(II-48)}$$

and

$$\frac{\partial\Theta_{1\eta}}{\partial\hat{\tau}} = \frac{\partial^2\Theta_{1\eta}}{\partial\xi^2} - \frac{\partial\Theta_{1\eta}}{\partial\xi} - \upsilon_{1\eta}\frac{\partial\Theta^{\circ}}{\partial\xi} \qquad \text{(II-49)}$$

with boundary conditions

$$\Theta_{1\eta}(-\infty,\hat{\tau}) = 0, \quad \Theta_{1\eta}(0,\hat{\tau}) = \vartheta_{1\eta} \qquad \text{(II-50)}$$

and

$$\frac{\partial\Theta_{1\psi}}{\partial\hat{\tau}} = \frac{\partial^2\Theta_{1\psi}}{\partial\xi^2} - \frac{\partial\Theta_{1\psi}}{\partial\xi} - \upsilon_{1\psi}\frac{\partial\Theta^{\circ}}{\partial\xi} + e^{i\lambda\hat{\tau}}\zeta^{\circ} \qquad \text{(II-51)}$$

with boundary conditions

$$\Theta_{1\psi}(-\infty,\hat{\tau}) = 0, \quad \Theta_{1\psi}(0,\hat{\tau}) = \vartheta_{1\psi} \qquad \text{(II-52)}$$

Thus, in the linear context the problem has been decomposed into

Three separate problems: (a) steady-state burning with radiant deposition, (b) burning with constant radiant deposition and nonsteady pressure, and (c) burning with constant pressure and nonsteady radiant deposition. These will be considered in turn.

Equation II-47 can be rewritten as the first order differential equation

$$\frac{d}{d\xi}\left(\frac{d\theta^\circ}{d\xi}\right) - \left(\frac{d\theta^\circ}{d\xi}\right) = -\zeta^\circ \tag{II-53}$$

The solution of this equation, noting that $d\theta^\circ/d\xi = 1$ at $\xi = 0$, is

$$\frac{d\theta^\circ}{d\xi} = e^{\xi} - e^{\xi} G(\xi) \tag{II-54}$$

where

$$G(\xi) = \int_0^{\xi} \zeta^\circ(\epsilon)\, e^{-\epsilon}\, d\epsilon \tag{II-55}$$

When there is no radiation ($\zeta^\circ \equiv 0$), $G = 0$ and the Michelson distribution is recovered.

Substitution of (II-54) into (II-49) yields

$$\frac{\partial \theta_{1\eta}}{\partial \tau} = \frac{\partial^2 \theta_{1\eta}}{\partial \xi^2} - \frac{\partial \theta_{1\eta}}{\partial \xi} - e^{\xi} \upsilon_{1\eta} + e^{\xi} \upsilon_{1\eta} G \tag{II-56}$$

Let $(\ )_{1\eta} = (\hat{\ })_{1\eta} e^{i\gamma\tau}$, then (II-56) becomes

$$\frac{d^2\hat{\theta}_{1\eta}}{d\xi^2} - \frac{d\hat{\theta}_{1\eta}}{d\xi} - i\gamma\hat{\theta}_{1\eta} = e^{\xi}\hat{\upsilon}_{1\eta} - e^{\xi}\hat{\upsilon}_{1\eta} G \tag{II-57}$$

Take $\hat{\theta}_{1\eta} = \hat{\theta}_H + \hat{\theta}_{P1} + \hat{\theta}_{P2}$ * where $\hat{\theta}_H$, $\hat{\theta}_{P1}$, and $\hat{\theta}_{P2}$ are solutions of

$$\frac{d^2\hat{\theta}_H}{d\xi^2} - \frac{d\hat{\theta}_H}{d\xi} - i\gamma\hat{\theta}_H = 0 \tag{II-58}$$

$$\frac{d^2\hat{\theta}_{P1}}{d\xi^2} - \frac{d\hat{\theta}_{P1}}{d\xi} - i\gamma\hat{\theta}_{P1} = \hat{\upsilon}_{1\eta} e^{\xi} \tag{II-59}$$

$$\frac{d^2\hat{\theta}_{P2}}{d\xi^2} - \frac{d\hat{\theta}_{P2}}{d\xi} - i\gamma\hat{\theta}_{P2} = \hat{\upsilon}_{1\eta} e^{\xi} G \tag{II-60}$$

*This form puts radiant effects into $\hat{\theta}_{P2}$.

respectively. The general solution of II-58 is[21]

$$\hat{\Theta}_H = Ae^{z_1\xi} + Be^{z_2\xi} \tag{II-61}$$

where z_1, z_2 are roots of the characteristic equation

$$z_1, z_2 = \left(1 \pm \sqrt{1 + 4i\gamma}\right)/2 \tag{II-62}$$

Since $\hat{\Theta}_H$ must be bounded at $\xi = -\infty$, $B = 0$ and

$$\hat{\Theta}_H = Ae^{z_1\xi} \tag{II-63}$$

where $z_1 = z_r + iz_i$ is complex. Algebraic manipulation and use of the quadratic formula yields

$$z_i = \sqrt{\left(\sqrt{1 + 16\gamma^2} - 1\right)/8} \tag{II-64}$$

$$z_r = (1 + \gamma/z_i)/2 \tag{II-65}$$

The solution of (II-59) can be found with the method of undetermined coefficients[21]. Let $\hat{\Theta}_{P1} = Ce^{\xi}$ where C is the undetermined coefficient. Substitution into (II-59) yields

$$C = i\hat{v}_{1\eta}/\gamma \tag{II-66}$$

Whence

$$\hat{\Theta}_{P1} = i\hat{v}_{1\eta}e^{\xi}/\gamma \tag{II-67}$$

The solution of (II-60) can be found by the variation of parameters method[21]. Let

$$\hat{\Theta}_{P2} = C(\xi)e^{\gamma_1 \xi} \tag{II-68}$$

Substitution into (II-60) yields

$$\frac{d^2C}{d\xi^2} + (2\gamma_1 - 1)\frac{dC}{d\xi} = -\hat{\upsilon}_{1\eta}\, e^{\xi}\, G \tag{II-69}$$

Taking $C' = dC/d\xi$ as the independent variable transforms (II-69) into a first order equation for C'. Integration yields

$$e^{(2\gamma_1 - 1)\xi}\, C' = -\hat{\upsilon}_{1\eta}\int_0^{\xi} e^{\gamma_1 \epsilon}\, G(\epsilon)\, d\epsilon + C'(0) \tag{II-70}$$

A second integration gives

$$C = -\hat{\upsilon}_{1\eta}\int_0^{\xi} e^{(2\gamma_1 - 1)\varphi}\int_0^{\varphi} e^{\gamma_1 \epsilon}\, G(\epsilon)\, d\epsilon\, d\varphi + C'(0)\xi + C(0) \tag{II-71}$$

Since a particular solution only is required, $C'(0)$ and $C(0)$ can both be set to zero. Therefore,

$$\hat{\Theta}_{P2} = e^{\gamma_1 \xi}\, \hat{\upsilon}_{1\eta}\, H(\xi) \tag{II-72}$$

where

$$H(\xi) = -\int_0^{\xi} e^{(2\gamma_1 - 1)\varphi}\int_0^{\varphi} e^{\gamma_1 \epsilon}\, G(\epsilon)\, d\epsilon \tag{II-73}$$

Consequently,

$$\hat{\Theta}_{1\eta} = e^{\gamma_1 \xi}(A + \hat{\upsilon}_{1\eta} H) + i\hat{\upsilon}_{1\eta}\, e^{\xi}/\gamma \tag{II-74}$$

Since $\vartheta_{1\eta} = \Theta_{1\eta}(\xi=0)$ (note that $H(0) = G(0) = 0$)

$$\vartheta_{1\eta} = A + i\hat{v}_{1\eta}/\gamma \tag{II-75}$$

By definition $\varphi = f/f^\circ = [(\partial\theta/\partial\xi)/(\partial\theta^\circ/\partial\xi)]$. From II-54 and -55, $f^\circ = 1$. Thus,

$$\varphi = 1 + \varphi_{1\eta} = (\partial\theta_{1\eta}/\partial\xi)_{\xi=0} \tag{II-76}$$

Differentiating II-74 (employ II-73 and Liebnitz's rule to find $(dH/d\xi)_{\xi=0} = 0$ and substituting into II-76 yields

$$\hat{\varphi}_{1\eta} = A z_1 + i\hat{v}_{1\eta}/\gamma - 1 \tag{II-77}$$

For steady-state burning without crossflow the functional dependencies $u^\circ = u^\circ(p, T_o^*)$ and $T_s^\circ = T_s^\circ(p, T_o^*)$ can be established experimentally. Therefore, the functions

$$k^* = (T_s^\circ - T_o^*)(\partial \ln u^\circ/\partial T_o^*)_p \quad , \quad r^* = (\partial T_s^\circ/\partial T_o^*)_p$$

$$\nu^* = (\partial \ln u^\circ/\partial \ln p)_{T_o^*} \quad , \quad \mu^* = (T_s^\circ - T_o^*)^{-1}(\partial T_s^\circ/\partial \ln p)_{T_o^*} \tag{II-78}$$

can also be established. To utilize the Z-N method one needs derivatives with respect to $\ln p$ and $\ln f^\circ$ because of the universality of the functions $u^\circ(p, f^\circ)$ and $T_s(p, f^\circ)$ for both steady and nonsteady conditions. Since

$$\left(\frac{\partial[\,]}{\partial \ln p}\right)_{f^\circ} = \frac{\partial([\,], \ln f^\circ)}{\partial(\ln p, \ln f^\circ)} = \frac{\partial([\,], \ln f^\circ)}{\partial(\ln p, T_o^*)} \Big/ \frac{\partial(\ln p, \ln f^\circ)}{\partial(\ln p, T_o^*)}$$

$$\left(\frac{\partial[\,]}{\partial \ln f^\circ}\right)_{p} = \frac{\partial([\,], \ln p)}{\partial(\ln f^\circ, \ln p)} = \frac{\partial([\,], \ln p)}{\partial(\ln p, T_o^*)} \Big/ \frac{\partial(\ln f^\circ, \ln p)}{\partial(\ln p, T_o^*)} \tag{II-79}$$

conversion into the "universal form" requires the partial derivatives $(\partial \ln f^\circ/\partial T_o^*)_p$ and $(\partial \ln f^\circ/\partial \ln p)_{T_o^*}$. Equation II-35 gives $f^\circ(u^\circ, T_s^\circ, T_o^*)$. Differentiation of II-35 then yields (with II-78)

$$(T_s^\circ - T_o^*)(\partial \ln f^\circ/\partial T_o^*)_p = k^* + r^* - 1$$

$$(\partial \ln f^\circ/\partial \ln p)_{T_o^*} = \nu^* + \mu^* \tag{II-80}$$

With these relations and II-78 and -79

$$
\begin{aligned}
(\partial \ln u / \partial \ln p)_f &= [\nu^*(r^*-1) - \mu^* k^*]/[k^* + r^* - 1] \\
(T_s^\circ - T_o^*)^{-1}(\partial T_s / \partial \ln p)_f &= [\mu^*(k^*-1) - \nu^* r^*]/[k^* + r^* - 1] \\
(\partial \ln u / \partial \ln f)_p &= k^*/[k^* + r^* - 1] \\
(T_s^\circ - T_o^*)^{-1}(\partial T_s / \partial \ln f^\circ)_p &= r^*/[k^* + r^* - 1]
\end{aligned}
\tag{II-81}
$$

The Jacobian

$$\delta^* = \partial(T_s^\circ, \ln u^\circ)/\partial(T_o^*, \ln p) = \nu^* r^* - \mu^* k^* \tag{II-82}$$

Since $\upsilon = \upsilon(\varphi, \eta)$ and $\vartheta = \vartheta(\varphi, \eta)$ [dimensionless form of $u^\circ(f^\circ, p)$ and $T_s^\circ(f^\circ, p)$ $T_s^\circ(f^\circ, p)$]

$$\upsilon_1 = (\partial \upsilon / \partial \varphi)_\eta \varphi_1 + (\partial \upsilon / \partial \eta)_\varphi \eta_1 \tag{II-83}$$

$$\vartheta_1 = (\partial \vartheta / \partial \varphi)_\eta \varphi_1 + (\partial \vartheta / \partial \eta)_\varphi \eta_1 \tag{II-84}$$

With the definitions for $\upsilon, \vartheta, \eta, \varphi$

$$
\begin{aligned}
(\partial \upsilon / \partial \eta)_\varphi &= (\upsilon / \eta)(\partial \ln u / \partial \ln p)_f \\
(\partial \upsilon / \partial \varphi)_\eta &= (\upsilon / \varphi)(\partial \ln u / \partial \ln f)_p \\
(\partial \vartheta / \partial \eta)_\varphi &= [\eta(T_s^\circ - T_o^*)]^{-1}(\partial T_s / \partial \ln p)_f \\
(\partial \vartheta / \partial \varphi)_\eta &= [\varphi(T_s^\circ - T_o^*)]^{-1}(\partial T_s / \partial \ln f)_p
\end{aligned}
\tag{II-85}
$$

Therefore, neglecting second order terms

$$\upsilon_1 = (\delta^* - \nu^*)\eta_1/(k^* + r^* - 1) + k^* \varphi_1/(k^* + r^* - 1)$$

$$\vartheta_1 = r^* \varphi_1/(k^* + r^* - 1) + (\delta^* + \mu^*)\eta_1/(k^* + r^* - 1) \qquad \text{(II-86)}$$

With II-75, -77, and -86 there are four equations and five unknowns ($\vartheta_1, \varphi_1, \eta_1, \upsilon_1, A$). Consequently, the ratio υ_1/η_1 can be solved for in terms of quantities that can be computed from $\mu^\circ(p, T_0^*)$ and $T_s^\circ(p, T_0^*)$ data. Since υ_1/η_1 is precisely the pressure coupled response function, this is the result desired.

Examination of II-75, -77, and -85 show that none of these equations depends explicitly upon the radiant energy deposition. Consequently, it must be concluded that the effects of steady radiant energy deposition in the non-reactive solid can always be accounted for by employing the radiation augmented initial temperature T_0^*! That is the pressure coupled response at p, T_0, J_s is that at $p, T_0^*, J_s = 0$. This situation was deduced on physical grounds for the special case $\ell_R \gg \kappa/\mu^\circ$. This work shows this to be the case in general.

REFERENCES

1. Edwards, G. , Gale, H. , and Kennedy, D. , "Outlook for Solid Rocket Motors," Astronautics and Aeronautics, September 1977.

2. Kruse, R. B. , Glick, R. L. , and Cohen, N. S. , "Stability Aspects of Prototype RS Mk 36 Motors," paper presented at 15th JANNAF Combustion Meeting, September 1978.

3. Culick, F. E. C. , ed. , "T-burner Testing of Metallized Solid Propellants," AFRPL-TR-74-28, October 1974.

4. Brown, R. S. , et. al. , "Combustion Instability Study of Solid Propellants," CPIA Publication 243, Vol. II, pp. 131-161.

5. Beckstead, M. W. , Derr, R. L. , and Price, C. F. , "A Model of Composite Solid Propellant Combustion Based on Multiple Flames," AIAAJ, 8, 12, 2200-2207, 1970.

6. Miller, R. R. , et. al. , "Control of Solids Distribution in HTPB Propellants," AFRPL-TR-78-14, April 1978.

7. Glick, R. L. and Condon, J. A. , "Statistical Combustion Modeling - The Effect of Additives," CPIA Publication 292, Vol. I, pp. 341-378, December 1977.

8. Condon, J. A. and Osborn, J. R. , "The Effect of Oxidizer Particle Size Distribution on the Steady and Nonsteady Combustion of Composite Propellants," AFRPL-TR-78-17, June 1978.

9. Condon, J. A. , Glick, R. L. , and Osborn, J. R. , "Statistical Analysis of Polydisperse, Heterogeneous Propellant Combustion: Nonsteady State," CPIA Publication 281, Vol. II, 1976.

10. Cohen, N. S. , et. al. , "Design of a Smokeless Solid Rocket Motor Emphasizing Combustion Stability," CPIA Publication.

11. Summerfield, M. , et. al. , "Theory of Dynamic Extinguishment of Solid Propellants with Special Reference to Nonsteady Heat Feedback Law," AIAA Paper 70-667.

12. Tien, C. L. and Lienhard, J. H. , Statistical Thermodynamics, (Holt, Rinehart and Winston, Inc. , 1971), p. 212.

13. Novozhilov, B. V., "Nonstationary Combustion of Solid Rocket Fuels," FTD-MT-24-317-74, 1974.

14. Glick, R. L. and Condon, J. A., "Statistical Analysis of Polydisperse, Heterogeneous Propellant Combustion: Steady-State," CPIA Publication 281, Vol. II, 1976.

15. Renie, J. P., Condon, J. A., and Osborn, J. R., "Oxidizer Distribution Effects," CPIA Publication 292, Vol, I, pp. 325-340, December 1977.

16. Beddini, R. A., "Reacting Turbulent Boundary Layer Approach to Solid Propellant Erosive Burning," AIAA Journal, Vol. 16, No. 9, pp. 898-905, September 1978.

17. Condon, J. A. and Osborn, J. R., "The Effect of Oxidizer Particle Size Distribution on the Steady and Nonsteady Combustion of Composite Propellants," AFRPL-TR-78-17, June 1978.

18. Culick, F. E. C., "A Review of Calculations for Unsteady Burning of a Solid Propellant," AIAA Journal, Vol. 6, No. 12, pp. 2241-2255, December 1968.

19. Sparrow, E. M. and Cess, R. D., Radiation Heat Transfer, (Brooks/Cole Publishing Co., Belmont, Ca., 1970).

20. Cantrell, R. H., et. al., "Effects of Thermal Radiation on the Acoustic Response of Solid Propellants," AIAAJ, Vol. 3, No. 3, p. 418, March 1965.

21. Golomb, M. and Shanks, M., Elements of Ordinary Differential Equations, (McGraw-Hill, New York, 1950).

APPENDIX A

NOMENCLATURE

Latin Symbols

A, B	constants
c	specific heat or acoustic speed
C	constant or function
D	diameter
$\bar{D}$	weight mean diameter
erf	denotes the error function
e, exp	denotes the exponential
f	temperature gradient at x=o, $(dT/dX)_{x=o}$
F	direct interchange factor for radiant transfer
G	$\int_0^{\xi} \mathcal{J}^{\circ}(\epsilon)\, e^{-\epsilon}\, d\epsilon$
h	see Figure II-1
H	$-\int_0^{\xi} e^{(2\zeta_1-1)\varphi} \int_0^{\varphi} e^{\zeta_1 \epsilon}\, G(\epsilon)\, d\epsilon\, d\varphi$
i	$\sqrt{-1}$ or an index
I	denotes an integral (see I-13 to -16)
J	*radiant heat flux*
$\mathcal{J}$	radiant heat flow
κ	an index,
k^*	function defined by II-78
l	extinction depth for thermal radiation
m	interaction parameter (see I-3) or mass flux

APPENDIX A

(Cont.)

M	number of oxidizer modes in propellant
N	number of oxidizer particles on surface S_p
n	pressure exponent
p	pressure
r	radius, burning rate
r^*	function defined by II-78
R	see Figure II-1
R_p	pressure coupled response function
R_v	velocity coupled response function
S	surface area
t	time
T	temperature
T_o^*	$T_o + J_s / [\rho c \mathring{u}]$
T_o	initial propellant temperature
T_s	burningsurface temperature or burning rate
u	$(x - x_k)/(\sigma_k \sqrt{2})$ or burning rate
w	mass fraction
x	lnD or spatial coordinate normal to the mean burning surface
x	see Figure II-1
ζ_1, ζ_2	roots of II-62

APPENDIX A

(Cont.)

Special Symbols

α	$(T_0 - T_0^*)/(T_s^\circ - T_0^*)$
α_{ox}	mass fraction of oxidizer
γ	$\kappa/(u^\circ)^2$
δ^*	defined by II-82
ϵ	dummy variable of integration
φ	dummy variable of integration or temperature gradient ratio f/f°
ρ	density
μ^*	function defined by II-78
Φ	radiant energy deposition per unit depth
θ	nondimensional temperature
κ	thermal diffusivity
υ	burning rate ratio u/u°
ξ	non-dimensional distance $u^\circ x/\kappa$
τ	non-dimensional time $(u^\circ)^2 t/\kappa$
η	non-dimensional pressure p/p°
ψ	non-dimensional radiant energy deposition Φ/Φ°
Υ	volume fraction of oxidizer
Υ°	non-dimensional radiant energy deposition, $\Phi^\circ(\kappa/u^\circ)/[\rho c u^\circ(T_s^\circ - T_0^*)]$
ν^*	function defined by II-78

APPENDIX A

(Cont.)

ϑ	non-dimensional burning surface temperature,
σ	$(\partial \ln \bar{r} / \partial T_0)_p$ or standard deviation
$\overline{(\ \ )}$	denotes a spatially mean value or a value non-dimensionalized by the oxidizer particle diameter
*	denotes a pseudo-propellant property or conditions with $J_\lambda = 0$.
$(\ \ )^{\circ}$	denotes steady-state condition

Subscripts

b	denotes binder
d	denotes diameter dependence
i	denotes ith value or imaginary part of complex number
k	denotes kth value
ox	denotes oxidizer
1	denotes a perturbation quantity
1η	denotes the portion of the perturbation quantity belonging to the pressure perturbation
1ψ	denotes the portion of the perturbation quantity belonging to the radiant flux perturbation.
t	denotes total
p	denotes quantity based on planar area S_p

APPENDIX A

(Cont.)

o	denotes J_s=o condition
r	denotes the reactive portion
s	denotes conditions at burning surface
S	denotes the area the function pertains to

APPENDIX B

FORTRAN IV CODE FOR EXTRACTING PSEUDO-PROPELLANT RATES FOR SPECIFIED M

```
      EXTERNAL MODER2,MODEN2,A1,A2,A3
      DIMENSION NM(8),HEAD(20),P(5),RMA(8),IPOINT(16)
      COMMON/MADER/II,JJ,ALFA(8,50),R(50,5),N(50),RC(50),ALFAT(50),
     1          RM(8,5),NC(50),K,ERR(50),ERN(50)
      COMMON /BLK/WMD(8),SD(8),    AI(8),AJ(25),AK(8),U(50),
     1          XMAX(50),XMIN(50),RHOT(50),RHOX,RHOB,API,SEEJ,
     2          C(50),RA(17),NI,AN(8),DIA,SIG,SDLN(8),WMDLN(8),TO
      COMMON /MAN/ E1(8,15),E2(8,15),E3(8,15),E4(8,15),ELEM1(21,8,15),
     1          ELEM2(21,8,15),ELEM3(21,8,15),ELEM4(21,8,15),X(16),I2
      REAL N,NM,NC
C R(J,K)    EXPERIMENTAL BURN RATES FOR THE JTH FORMULATION AND P(K)
C N(J)      EXPERIMENTAL PRESSURE EXPONENT FOR THE JTH FORMULATION AND
C           P(1)
C RC(J)     CALCULATED BURN RATE FOR THE JTH FORMULATION AND P(K)
C NC(J)     CALCULATED EXPONENT FOR THE JTH FORMULATION AND P(K)
C ERR1      STANDARD DEVIATION OF RC FROM R FOR P(K)
C ERR2      STANDARD DEVIATION OF NC FROM N FOR P(K)
C RM(I,K)   MODAL BURNING RATE FOR ITH MODE  AND P(K)
C NM(I)     PRESSURE EXPONENT FOR THE ITH MODE AND P(1)
C ALFA(I,J) MASS FRACTION OF ITH MODE OXIDIZER IN JTH FORMULATION
C ALFAT(J)  TOTAL OXIDIZER CONTENT OF JTH FORMULATION
C II        NUMBER OF OX MODES < 8
C JJ        NUMBER OF FORMULATIONS < 50
C KK        NUMBER PRESSURES RATE DATA AVAILABLE < 5
C ERR(J)    ERROR BETWEEN R(J,K) AND RC(J) AT P(K)
C ERN(J)    ERROR BETWEEN N(J) AND NC(J) FOR P(1)
C
C THEORY ASSUMES THAT
C       R(J)=SUM(ALFA(I,J)*RM(I))/SUM(ALFA(I,J))
C       N(J)=SUM(ALFA(I,J)*RM(I)*NM(I))/SUM(ALFA(I,J)*RM(I))
C
C KEN HERREN    MARCH 27, 1978
C
C INPUT JOB HEADING AND PRINT OUT THAT HEADING
C
      NI=6
      API=3.14159
      RHOB=0.91
      RHOX=1.95
    1 READ(5,10,END=210) HEAD
   10 FORMAT(20A4)
      WRITE(6,11) HEAD
   11 FORMAT(1H1,20A4,//2H *20X,'OX MASS FRACTION DATA',21X,2H**,21X
     1,'EXPONENT,RATE DATA',23X,1H*,//3X,'MODE 1',2X,'MODE 2',2X,'MODE3'
     2,2X,'MODE 4',2X,'MODE 5',2X,'MODE 6',2X,'MODE 7',2X,'MODE 8',3X,
     3'N(P1)',3X,'R(P1)',3X,'R(P2)',3X,'R(P3)',3X,'R(P4)',3X,'R(P5)',/)
C
C INPUT DATA
C
      READ(5,20) II,JJ,KK,(P(K),K=1,KK)
   20 FORMAT(3I2,5F5.0)
      DO 60 J=1,JJ
      READ(5,30) (ALFA(I,J),I=1,8),N(J),(R(J,K),K=1,KK)
   30 FORMAT(14F5.4)
C
C OUTPUT INPUT DATA
C
      WRITE(6,40) (ALFA(I,J),I=1,II)
   40 FORMAT(1H ,8F8.4)
      WRITE(6,50) N(J),(R(J,K),K=1,KK)
```

```
   50 FORMAT(1H+,64X,6F8.4)
   60 CONTINUE
      READ(5,25) (WMD(I),I = 1,II)
 25   FORMAT(8F7.3)
      READ(5,27) (SD(I),I=1,II)
   27 FORMAT(8F5.3)
      WRITE(6,26) (WMD(I),SD(I),I=1,II)
 26   FORMAT(1X,2F10.3)
      READ(5,29) (RA(I),I=1,13)
 29   FORMAT(3E12.4)
      READ(5,31) (IPOINT(NN),NN=2,11),I2,IJKLM
 31   FORMAT(12I2)
      WRITE(6,32) RA(I2+2)
 32   FORMAT(1H0,'THE CURRENT N = ',F8.4)
C
C RESET KPRINT FOR NM(I) DETERMINATION
C
      KPRINT=1
C
C COMPUTE ALFAT(J)
C
      DO 67 J=1,JJ
      ALFAT(J)=0.0
         DO 63 I=1,II
         ALFAT(J)=ALFAT(J)+ALFA(I,J)
         RHOT(J)=RHOT(J)+ALFA(I,J)/RHOX
   63    CONTINUE
         RHOT(J)=1./(RHOT(J)+(1.-ALFAT(J))/RHOB)
   67 CONTINUE
C
C FIND RM(I,K) FOR EACH P(K)
C
      DO 200 K =1,KK
C
C SET INITIAL RM(I,K)
C
      WRITE(6,68)
 68   FORMAT(1H0,'MODAL INTEGRALS ARE'/11X,'XMAX',11X,'XMIN',
     1         8X,'DIAMETER',8X,'SIGMA',8X,'INTEGRAL')
      DO 70 I = 1,II
      WMDLN(I)=ALOG(WMD(I))
      SDLN(I)=ALOG(SD(I))
      XMAX(I)=WMDLN(I)+3.*SDLN(I)
      XMIN(I)=WMDLN(I)-3.*SDLN(I)
      XY1=XMAX(I)
      XY2=XMIN(I)
      DIA=WMDLN(I)
      SIG=SDLN(I)
      AI(I)=SIMP(XY1,XY2,A2,N1)
      WRITE(6,69) XY1,XY2,DIA,SIG,AI(I)
 69   FORMAT(1H ,5(3X,F12.5))
         RMA(I)=R(1,K)
         IF(K .EQ. 1) AN(I)=N(1)
   70    CONTINUE
C
C     COMPUTE THE FORMULATION INTEGRALS
C
      XSTART=WMDLN(1)+0.1+3.*SDLN(1)
      XEND  =WMDLN(8)-0.1-3.*SDLN(8)
      XDEL  =(XEND-XSTART)/31.
```

```
      IPOINT(1)=0
C
      DO 837 IL=1,I2
         X(IL)=XSTART + FLOAT(IPOINT(IL))*XDEL
  837 CONTINUE
      ILT=I2+1
      IG=ILT+1
      X(ILT )=XEND
      WRITE(6,838) (X(IJK),IJK=1,ILT)
  838 FORMAT(1H0,8(2X,F12.5))
      DO 1000 J=1,JJ
         SUM=0.
         DO 800 KEN=1,I1
            DO 900 I=1,I2
               Y1=X(I+1)
               IF(ALFA(KEN,J).EQ.0.) GO TO 3100
               Y2=X(I)
               DIA=WMDLN(KEN)
               SIG=SDLN(KEN)
               E1(KEN,I)=-SIMP(Y1,Y2,A1,N1)
               E2(KEN,I)=-SIMP(Y1,Y2,A2,N1)
               AZ1=((X(I+1)-WMDLN(KEN))/SDLN(KEN))**2
               BZ1=((X(I)   -WMDLN(KEN))/SDLN(KEN))**2
               AZ=0.
               BZ=0.
               IF(AZ1.LE.50.0) AZ=EXP(-0.5*AZ1)
               IF(BZ1.LE.50.0) BZ=EXP(-0.5*BZ1)
               E3(KEN,I)=     BZ-AZ
               E4(KEN,I)=     BZ*EXP((RA(IG)-3.)*X(I))-
     1                 AZ*EXP((RA(IG)-3.)*X(I+1))
               Z=X(I+1)-X(I)
               T=(X(I)-WMDLN(KEN))/Z
               ELEM1(J,KEN,I)=((1.+T)*E1(KEN,I)/SDLN(KEN)  + E3(KEN,I)/Z)
     1                    *ALFA(KEN,J)/2.506627
               ELEM2(J,KEN,I)=(-1.*T*E1(KEN,I)/SDLN(KEN)  - E3(KEN,I)/Z)*
     1                    ALFA(KEN,J)/2.506627
            ELEM3(J,KEN,I)=((1.+T-((RA(IG)-3.)*SDLN(KEN))/Z)*E2(KEN,I)
     1         /SDLN(KEN) + E4(KEN,I)/Z)*ALFA(KEN,J)/2.506627
               ELEM4(J,KEN,I)=(-1.*(T-((RA(IG)-3.)*SDLN(KEN))/Z)*
     1         E2(KEN,I)/SDLN(KEN)-E4(KEN,I)/Z)*ALFA(KEN,J)/2.506627
               GO TO 3500
 3100          CONTINUE
               ELEM1(J,KEN,I)=0.
               ELEM2(J,KEN,I)=0.
               ELEM3(J,KEN,I)=0.
               ELEM4(J,KEN,I)=0.
 3500          CONTINUE
  900       CONTINUE
            SUM=SUM + ALFA(KEN,J)*AI(KEN)/SDLN(KEN)
  800    CONTINUE
         AJ(J)=SUM/2.506627
         IF(IJKLM.EQ.1) GO TO 1649
         WRITE(6,1600) J,AJ(J)
         WRITE(6,1650) ((ELEM1(J,J1,J2),J2=1,I2),J1=1,8)
         WRITE(6,1650) ((ELEM2(J,J1,J2),J2=1,I2),J1=1,8)
         WRITE(6,1650) ((ELEM3(J,J1,J2),J2=1,I2),J1=1,8)
         WRITE(6,1650) ((ELEM4(J,J1,J2),J2=1,I2),J1=1,8)
 1600    FORMAT(1H0,5X,'INTEGRAL VALUES FOR THE # ',I3,' FORMULATION
     1    ARE',5X,'AJ SUB J = ',E12.5)
 1650    FORMAT(1H ,11F8.4)
```

```
 1649      CONTINUE
 1000   CONTINUE
C
        IF(IJKLM.EQ.1) GO TO 80
        DO 1234 JCNT=1,JJ
        WRITE(6,1235) ((E1(KCNT,ICNT),ICNT=1,I2),KCNT=1,II)
        WRITE(6,1235) ((E2(KCNT,ICNT),ICNT=1,I2),KCNT=1,II)
        WRITE(6,1235) ((E3(KCNT,ICNT),ICNT=1,I2),KCNT=1,II)
        WRITE(6,1235) ((E4(KCNT,ICNT),ICNT=1,I2),KCNT=1,II)
 1235   FORMAT(1H ,11F8.4)
C
 1234   CONTINUE
C FIND OPTIMAL RM(I,K)
C
   80 CALL PATSH(RA,ERR1,ILT,10.0,0.001,50,1,MODER2)
           DO 90 I=1,II
   90      RM(I,K)=RA(I)
C
C NEED FIND NM(I) ?
C
        IF(K .GT. 1) KPRINT=2
        IF(N(1) .EQ. 0.0) KPRINT=2
        IF(KPRINT .EQ. 2) GO TO 100
C
C FIND OPTIMAL N(I)
C
        CALL PATSH(AN,ERR2,II,5.0,0.001,50,-1,MODEN2)
        DO 95 I = 1,II
 95      NM(I)=AN(I)
C
C OUTPUT COMPUTED RESULTS THIS P(K)
C
  100 WRITE(6,110) HEAD
  110 FORMAT(1H1,20A4)
      WRITE(6,115) P(K),ERR1,ERR2
  115 FORMAT(1H0,3HP =,F6.1,4H PSI,5X,'RATE STD ERR=',1PE11.4,5X,'EXPONE
     1NT STD ERR=',1PE11.4///2H *,16X,'COMPUTED MODAL RATES,IN/SEC',18X,
     22H**,18X,'COMPUTED MODAL EXPONENTS',21X,1H*,//4X,'RM1',5X,'RM2',5X
     3,'RM3',5X,'RM4',5X,'RM5',5X,'RM6',5X,'RM7',5X,'RM8',5X,'NM1',5X,
     4'NM2',5X,'NM3',5X,'NM4',5X,'NM5',5X,'NM6',5X,'NM7',5X,'NM8',//)
      WRITE(6,120) (RM(I,K),I=1,II)
  120 FORMAT(1H , 8F8.4)
      IF(KPRINT .EQ. 1) WRITE(6,130) (NM(I),I=1,II)
  130 FORMAT(1H+,64X, 8F8.4)
      WRITE(6,140)
  140 FORMAT(2H0*,10X,'COMPARISON THEORY/EXPERIMENT',9X,1H*//5X,'R',7X,
     1'RC',5X,'ERR',6X,'N',7X,'NC',5X,'ERN',/)
         DO 180 J=1,JJ
         WRITE(6,150) P(J,K),RC(J),ERR(J)
  150    FORMAT(1H  ,3F8.4)
         IF(KPRINT .EQ. 1) WRITE(6,160) N(J),NC(J),ERN(J)
  160    FORMAT(1H+ ,24X,3F8.4)
  180    CONTINUE
      KPRINT=1
  200 CONTINUE
      GO TO 1
  210 STOP
      END
```

```
      SUBROUTINE MODEN2(AN,ERR2)
      EXTERNAL  A1,A2,A3
      DIMENSION NM(8),AN(8)
      COMMON/MADER/II,JJ,ALFA(8,50),R(50,5),N(50),RC(50),ALFAT(50)
     1           ,RM(8,5),NC(50),K,ERR(50),ERN(50)
      COMMON/BLK/WMD(8),SD(8),     AI(8),AJ(25),AK(8),U(50),
     1             XMAX(50),XMIN(50),RHOT(50),RHOX,RHOB,API,SEEJ,
     2             C(50),SA(17),N1,BN(8),DIA,SIG,SDLN(8),WMDLN(8),TQ
      REAL N,NM,NC
C
C THIS SUBROUTINE FINDS THE STANDARD DEVIATION BETWEEN N(J) AND NC(J)
C
C    N(J)          EXPERIMENTAL EXPONENT FOR JTH FORMULATION AT P(1)
C   NC(J)          THEORETICAL EXPONENT FOR JTH FORMULATION
C   RM(I,K)        BURNING RATE FOR THE ITH MODE AT P(K)
C   NM(I)          EXPONENT FOR THE ITH MODE AT P(1)
C   ALFA(I,J)      MASS FRACTION OF ITH OX MODE IN JTH FORMULATION
C   ALFAT(J)       TOTAL MASS FRACTION OF OX IN JTH FORMULATION
C   II             NUMBER OF MODES <8
C   JJ             NUMBER OF FORMULATIONS < 50
C   ERN(J)         ERROR BETWEEN N(J) AND NC(J)
C   ERR2           STANDARD ERROR OF ESTIMATE FOR DATA SET N AND NC
C
C     KEN HERREN   MARCH 28,1978
C
C
      DO 15 I=1,8
   15 BN(I)=AN(I)
    5 ERR2=0.0
   10 DO 30 J=1,JJ
      NC(J)=0.0
        DO 25 I=1,II
      IF(WMD(I).NE.0.) GO TO 23
      TNCALC=0.
      GO TO 24
   23 YX=XMAX(I)
      YY=XMIN(I)
      DIA=WMDLN(I)
      SIG=SDLN(I)
      AK(I)=SIMP(YX,YY,A3,N1)
      TNCALC=ALFA(I,J)*AK(I)/SDLN(I)
   24 CONTINUE
   25 NC(J)=NC(J)+TNCALC
      NC(J)=NC(J)*0.39894
C CALCULATE EXPONENT USING MEASURED RATE
      NC(J)=NC(J)/ALFAT(J)/R(J,1)
C CALCULATE EXPONENT USING CALCULATED RATE
C     NC(J)=NC(J)/ALFAT(J)/RC(J)
C CALCULATE ABSOLUTE ERROR
C     ERN(J)=N(J)-NC(J)
C CALCULATE RELATIVE ERROR
      ERN(J)=(N(J)-NC(J))/N(J)
   30 ERR2=ERR2 + ERN(J)*ERN(J)
      ERR2=SQRT(ERR2/JJ)
      RETURN
      END
```

```
      SUBROUTINE MODER2(RA,ERR1)
      EXTERNAL   A1,A2,A3
      COMMON/MADER/II,JJ,ALFA(8,50),R(50,5),N(50),RC(50),ALFAT(50)
     1             ,RM(8,5),NC(50),K,ERR(50),ERN(50)
      COMMON/BLK/WMD(2),SD(8),     AI(8),AJ(25),AK(8),U(50),
     1            XMAX(50),XMIN(50),RHOT(50),RHOX,RHOB,API,SEEJ,
     2            C(50),SA(17),N1,BN(8),DIA,SIG,SDLN(8),WMDLN(8),TQ
      COMMON /MAN/ E1(8,15),E2(8,15),E3(8,15),E4(8,15),ELEM1(21,8,15),
     1            ELEM2(21,8,15),ELEM3(21,8,15),ELEM4(21,8,15),X(16),I2
      DIMENSION RMA(8),RA(17)
C THIS SUBROUTINE COMPUTES STANDARD DEVIATION BETWEEN R(J,K) AND RC(J)
C FOR P(K)
C WHERE
C  R(J,K)        EXPERIMENTAL BURNING RATE FOR JTH FORMULATION AT P(K)
C  RC(J)         THEORETICAL BURNING RATE FOR JTH FORMULATION AT P(K)
C  RMA(I)        BURNING RATE FOR ITH MODE OF FORMULATION AT P(K)
C  ALFA(I,J)     MASS FRACTION OF ITH MODE OX IN JTH FORMULATION
C  ALFAT(J)      TOTAL OX MASS FRACTION IN JTH FORMULATION
C  II            NUMBER OF OX MODES < 8
C  JJ            NUMBER OF FORMULATIONS < 50
C  ERR(J)        ERROR BETWEEN R(J,K) AND RC(J) AT P(K)
C  ERR1          STANDARD ERROR OF ESTIMATE FOR DATA SET R AND RC
C
C     KEN HERREN    MARCH 27, 1978
C
C
      ILT=I2+1
      DO 5 I = 1,ILT
    5 SA(I)=RA(I)
   10 ERR1=0.00
      SUM1=0.
      DO 300 J=1,JJ
         RC(J)=0.
         SUME=0.
         SUMF=0.
         DO 330 I=1,I2
            SUM1=0.
            SUMA=0.
            SUMB=0.
            SUMC=0.
            SUMD=0.
            DO 360 KEN =1,II
               SUMA = SUMA + ELEM1(J,KEN,I)
               SUMB = SUMB + ELEM2(J,KEN,I)
               SUMC = SUMC + ELEM3(J,KEN,I)
               SUMD = SUMD + ELEM4(J,KEN,I)
  360       CONTINUE
            SUME = RA(I)*SUMA + RA(I+1)*SUMB + SUME
            SUMF = RA(I)*SUMC + RA(I+1)*SUMD + SUMF
  330    CONTINUE
         RC(J) = SUME + (1.-ALFAT(J))*SUMF/AJ(J)
C        WRITE(6,1000) SUMA,SUMB,SUMC,SUMD,SUME,SUMF
C1000 FORMAT(1H ,10X,6(2X,F12.5))
C COMPUTE ABSOLUTE ERROR
         ERR(J)=R(J,K)-RC(J)
C COMPUTE RELATIVE ERROR
C        ERR(J)=(R(J,K)-RC(J))/R(J,K)
         ERR1=ERR1+ERR(J)*ERR(J)
C        WRITE(6,35) ERR(J),R(J,K),RC(J),ERR1
C 35  FORMAT(1H ,4E12.5)
```

```
  300 CONTINUE
      ERR1=SQRT(ERR1/JJ)
      RETURN
      END
```

```
      SUBROUTINE PATSH(PSI,SSI,N,DELS,DLMIN,ITLIM,IPT,MERIT)
      DIMENSION PSI(25),PHI(25),THT(25),XFLG(25)
C
C     PRINTER AND HIGH SPEED CONSOLE DEVICE NUMBERS
C
      DATA ALFA/1.02/
C
C     FUNCTION F IS MINIMUM IMPROVEMENT REQUIRED OVER LAST BASEPOINT
C
      F(SSS)=SSS - ABS(SSS)*0.0001*CUT
C
C     PSI IS THE CURRENT BASE POINT
C     THT IS THE PREVIOUS BASE POINT
C     PHI IS THE TRIAL POINT
C     S   IS THE OBJECTIVE FUNCTION
C     IPT =  1 FOR DIAGNOSTIC PRINTOUT
C            0 FOR MINIMAL PRINTOUT
C           -1 FOR NO PRINTOUT
C
C
C     INITIALIZATION
C
      ITWICE=1
      DEL=DELS
      IF(IPT.GE.0)WRITE(6,604) DEL,DLMIN,ITLIM,IPT
      DO 705 I=1,N
  705 XFLG(I)=1.0
      ITER=0
      CUT=1.0
C
C     EVALUATE AT INITIAL BASE POINT
C
   10 CALL MERIT(PSI,SSI)
C
C     EXPLORE AROUND CURRENT BASEPOINT
C
   90 SSITST=F(SSI)
  100 S=SSI
      NPATM=0
      DO 101 I=1,25
  101 PHI(I)=PSI(I)
      ICALL=1
      IF(IPT.LT.0)GO TO 150
      WRITE(6,599)ITER
      WRITE(6,600) (PSI(J),J=1,N)
      WRITE(6,601)S,DEL
C
C     MAKE EXPLORATORY MOVE
C
      GO TO 150
C
C     IS THE PRESENT VALUE LESS THAN THE BASE POINT VALUE
C
  160 IF(S.LT.SSITST) GO TO 200
C
C     CUT STEP SIZE
C
      DEL=0.5*DEL
      IF(DEL.GT.DLMIN) GO TO 100
      IF(IPT.GE.0) WRITE(6,704)
```

```
      IF(CUT.LT.0.5) GO TO 702
C
C     START OVER WITH INITIAL DEL AND CURRENT BASE POINT
C
      CALL MERIT(PHI,SPI)
      IF(IPT.GE.0) WRITE(6,707)
      IF(ITWICE.EQ.0)RETURN
      DEL=DELS
      CUT=0.
      GO TO 90
C
C     SET NEW BASE POINT
C     MAKE PATTERN MOVE
C     EXPLORE AROUND PATTERN
C
  200 SSI=S
      SSITST=F(SSI)
      ITER=ITER + 1
      NPATM=NPATM + 1
      IF(ITER.GT.ITLIM)GO TO 700
      IF(IPT.LT.0)GO TO 203
      WRITE(6,599) ITER
      WRITE(6,599) NPATM
      WRITE(6,600) (PHI(I),I=1,N)
      WRITE(6,601) SSI,DEL
C
C     MAKE PATTERN MOVE
C
  203 DO 201 I=1,N
      THT(I)=PSI(I)
      PSI(I)=PHI(I)
  201 PHI(I)=PHI(I) + ALFA*(PHI(I) - THT(I))
      CALL MERIT(PHI,SPI)
      S=SPI
      IF(IPT.NE.1)GO TO 202
      WRITE(6,606) (PHI(I),I=1,N)
      WRITE(6,601) SPI,DEL
  202 ICALL=2
C
C     MAKE EXPLORATORY MOVE
C
      GO TO 150
C
C     IS THE PRESENT VALUE LESS THAN THE BASE POINT VALUE
C
  260 IF(S.LT.SSITST) GO TO 200
      GO TO 100
C
C     INTERNAL SUBROUTINE TO MAKE EXPLORATIONS ABOUT PHI
C
  150 DO 180 K=1,N
      PHIOLD=PHI(K)
      STEPK=0.05*PHIOLD
      IF(STEPK.EQ.0.0) STEPK=0.05
      STEPK=SIGN(STEPK*DEL,XFLG(K))
      PHI(K)=PHIOLD + STEPK
      CALL MERIT(PHI,SPI)
      IF(IPT.EQ.1)WRITE(6,602) ICALL,K,SPI,(PHI(L),L=1,N)
      IF(SPI.LT.S) GO TO 179
      XFLG(K)=-XFLG(K)
```

```
      PHI(K)=PHIOLD - STEPK
      CALL MERIT(PHI,SPI)
      IF(IPT.EQ.1) WRITE(6,602) ICALL,K,SPI,(PHI(L),L=1,N)
      IF(SPI.LT.S) GO TO 179
      PHI(K)=PHIOLD
      GO TO 180
  179 S=SPI
  180 CONTINUE
      GO TO  (160,260),ICALL
C
C
  700 IF(IPT.GE.0)WRITE(6,701)
  702 DO 703 I=1,N
  703 PSI(I)=PHI(I)
      IF(IPT.GE.0)WRITE(6,607)ITER
      RETURN
  599 FORMAT(' **** ',I5)
  600 FORMAT('   BASE PT ', 1P4(7E15.6,E15.6,/,T9))
  606 FORMAT('   PATTERN ', 1P4(7E15.6,E15.6,/,T9))
  601 FORMAT(6X,'OBJ',1PE15.6,5X,'DEL ',E15.6)
  602 FORMAT(1X,2I2,' OBJ  ',1PE14.6,' TRIAL  ',4(6E14.6, E14.6,/,T35))
  604 FORMAT('ODEL ',1PE15.6,',    DELMIN ',E15.6,1X,//,' ITLIM ',I6,',
     1 IPT ',I3)
  607 FORMAT(' TOTAL NUMBER OF NEW BASE POINTS (ITERATIONS)  ',I5)
  701 FORMAT('OSEARCH TERMINATED BECAUSE NUMBER OF ITERATIONS EXCEEDS
     1LIMIT.')
  704 FORMAT('OSEARCH TERMINATED BECAUSE STEP SIZE LESS THAN LIMIT.')
  707 FORMAT('0 STARTING OVER WITH CURRENT BASE POINT AND INITIAL DEL.')
      END
```

```
      FUNCTION A1(V)
      COMMON/BLK/WMD(8),SD(8),      AI(8),AJ(25),AK(8),U(50),
     1            XMAX(50),XMIN(50),RHOT(50),RHOX,RHOB,API,SEEJ,
     2            C(50),RA(17),N1,AN(8),DIA,SIG,SDLN(8),WMDLN(8),TQ
      W=((V-(DIA))/SIG)**2
      A1=0.
      IF(W.LE.50.0) A1=EXP(-0.5*W)
      RETURN
      END
```

```
      FUNCTION A2(V)
      COMMON/BLK/WMD(8),SD(8),     AI(8),AJ(25),AK(8),U(50),
     1            XMAX(50),XMIN(50),RHOT(50),RHOX,RHOB,API,SEEJ,
     2            C(50),RA(17),N1,AN(8),DIA,SIG,SDLN(8),WMDLN(8),TQ
      COMMON /MAN/ E1(8,15),E2(8,15),E3(8,15),E4(8,15),ELEM1(21,8,15),
     1            ELEM2(21,8,15),ELEM3(21,8,15),ELEM4(21,8,15),X(16),I2
      ILU=I2+2
      A2=0.
      W=((V-(DIA))/SIG)**2
      Y=RA(ILU)-3.
      IF(W.LE.50.)A2=EXP(V)**Y * EXP(-0.5*W)
      RETURN
      END
```

```
      FUNCTION A3(V)
      COMMON/MADER/II,JJ,ALFA(8,50),R(50,5),N(50),RC(50),ALFAT(50)
     1           ,RM(8,5),NC(50),K,ERR(50),ERN(50)
      COMMON/BLK/WMD(8),SD(8),     AI(8),AJ(25),AK(8),U(50),
     1           XMAX(50),XMIN(50),RHOT(50),RHOX,RHOB,API,SEEJ,
     2           C(50),RA(17),N1,AN(8),DIA,SIG,SDLN(8),WMDLN(8),TQ
C
      X=(EXP(V)/AN(3))**2
      B2=AN(1) + AN(2)/SQRT((1.-X)**2 + 4.*(AN(4)**2)*X)
      TP = RA(5)-3.
      TS = B2*TQ
       TR = ((V-DIA) /SIG)**2
       A3 = TS*EXP(-0.5*TR)
       RETURN
         END
```

```
  MILLER DATA SET SD-I-88-1,-25 (18% 24 MICRCN AL)
0821031000.500. 2000.
                .3        .3        .1   .656 .984 .6261.554                 -01
                .3   .1             .3   .803 .796 .4761.448                 -03
      .3             .1             .3   .764 .494 .3481.003                 -04
 .4                                 .3   .449 .317 .236 .440                 -05
                .3        .3   .1        .660 .976 .6191.545                 -06
                .3   .1        .3        .743 .927 .5661.524                 -08
      .3             .1        .3        .792 .479 .329 .990                 -09
 .4                            .3        .427 .290 .222 .401                 -10
                     .3   .4             .6201.105 .7181.697                 -11
           .3             .4             .653 .741 .5051.248                 -12
      .3             .1   .3             .719 .503 .367 .993                 -14
 .4                       .3             .566 .293 .222 .487                 -15
      .3        .3   .1                  .514 .441 .313 .639                 -16
           .3        .4                  .520 .665 .462 .951                 -17
           .4        .3                  .481 .582 .413 .805                 -18
      .3             .4                  .593 .523 .363 .826                 -19
 .4                  .3                  .575 .305 .231 .512                 -20
 .3   .3        .1                       .417 .299 .219 .390                 -21
 .3             .4                       .480 .379 .283 .550                 -22
      .4        .3                       .491 .399 .265 .523                 -23
 .4             .3                       .481 .323 .228 .444                 -25
  MILLER DATA SET SD-III-1,-25 (ZERO ADDITIVE)
0821031000.500. 2000.
          .3158     .1368          .4211 .9161.165 .6272.214                 -02
                    .5579          .3158 .6891.446 .8812.291                 -03
     .3158          .2421          .3158 .7971.168 .6321.909                 -04
.4211               .1368          .3158 .928 .870 .4711.704                 -05
               .3158.1368.3158.1053      .6211.160 .7371.744                 -06
               .3158.2421     .3158      .6921.096 .6801.774                 -08
     .3158          .2421     .3158      .7711.087 .6311.822                 -09
.4211               .1368     .3158      .841 .901 .5001.604                 -10
          .3158     .1368.4211           .6171.030 .6761.589                 -12
     .3158          .2421.3158           .613 .978 .6371.490                 -14
.4211               .1368.3158           .690 .706 .4491.169                 -15
     .3158     .3158.2421                .451 .561 .407 .761                 -16
          .3158     .5579                .474 .834 .6011.158                 -17
          .4211     .4526                .437 .718 .521 .955                 -18
     .3158          .5579                .529 .785 .5361.116                 -19
.4211               .4526                .610 .539 .368 .856                 -20
.3158.3158     .1053.1368                .430 .330 .240 .436                 -21
.3158          .4211.1368                .458 .524 .375 .708                 -22
     .4211     .3158.1368                .463 .469 .332 .630                 -23
     .3158     .4211.1368                .449 .536 .393 .732                 -24
.4211          .3158.1368                .528 .445 .304 .652                 -25
  MILLER DATA SET SD-IV-1,-25  (18% 90 MICRCN AL)
0820031000.500. 2000.
                .3        .3        .1   .6231.050 .7041.671                 -01
                .3   .1             .3   .696 .916 .5571.461                 -03
      .3             .1             .3   .848 .468 .3291.065                 -04
 .4                                 .3   .424 .298 .220 .397                 -05
                .3        .3   .1        .6131.037 .6551.533                 -06
                .3   .1        .3        .674 .951 .5771.475                 -08
      .3             .1        .3        .904 .476 .3111.089                 -09
 .4                            .3        .439 .266 .203 .373                 -10
           .3             .4             .595 .765 .5121.168                 -12
                     .4   .3             .6021.250 .8081.861                 -13
      .3             .1   .3             .708 .568 .3791.012                 -14
 .4                       .3             .612 .250 .205 .478                 -15
```

```
      .3             .3   .1                .478 .464 .322 .624                  -16
           .3             .4                .470 .667 .483 .927                  -17
           .4             .3                .456 .604 .433 .814                  -18
      .3                  .4                .604 .488 .343 .793                  -19
 .4                       .3                .630 .259 .193 .461                  -20
 .3   .3             .1                     .460 .309 .216 .408                  -21
 .3                  .4                     .565 .404 .270 .591                  -22
 .4                  .3                     .531 .232 .230 .480                  -25
  MILLER DATA SET SD-V-1,-25 (18% 6 MICRON AL)
0819031000. 500.2000.
                     .3        .3        .1 .574 .917 .6361.410                  -01
                     .3   .1             .3 .674 .812 .5221.327                  -03
      .3                  .1             .3 .583 .535 .382 .857                  -04
 .4                                      .3 .462 .355 .261 .495                  -05
                     .3        .3   .1      .592 .895 .5911.344                  -06
                     .3   .1        .3      .610 .869 .5651.310                  -08
      .3                  .1        .3      .556 .567 .403 .870                  -09
 .4                                 .3      .502 .357 .263 .527                  -10
 .4                            .3           .538 .348 .258 .544                  -15
      .3             .3   .1                .450 .481 .352 .656                  -16
           .3             .4                .439 .676 .508 .933                  -17
           .4             .3                .410 .616 .462 .815                  -18
      .3                  .4                .473 .527 .399 .768                  -19
 .4                       .3                .502 .347 .261 .523                  -20
 .3   .3             .1                     .433 .299 .221 .403                  -21
 .3                  .4                     .465 .407 .299 .569                  -22
      .4             .3                     .433 .420 .319 .583                  -23
      .3             .4                     .420 .469 .356 .637                  -24
 .4                  .3                     .513 .335 .242 .492                  -25
  MILLER DATA SET SD-VI-1,-25 (INCREASED SOLIDS, 21% 24 MICRON AL)
0506031000. 500.2000.
     .2957     .0986.2957                   .799 .726 .4381.327                  -14
.3943               .2957                   .800 .382 .253 .767                  -15
     .2957     .3943                        .645 .589 .390 .954                  -19
.3943          .2957                        .694 .372 .254 .665                  -20
.2957.2957.0986                             .457 .314 .229 .432                  -21
.3943     .2957                             .544 .402 .265 .563                  -25
  MILLER DATA SET SD-VII-1,-25 (18% 24 MICRON AL + 1% FEO)
0817031000. 500.2000.
               .2957     .2957.0986         .5391.303 .8421.778                  -06
               .2957.0986     .2957         .5611.285 .8201.784                  -08
     .2957          .0986     .2957         .6551.219 .6871.703                  -09
.3943                         .2957         .663 .964 .5201.303                  -10
          .2957          .3943              .5571.146 .7401.601                  -12
     .2957          .0986.2957              .5311.039 .6871.435                  -14
.3943                    .2957              .597 .762 .4951.132                  -15
          .2957     .3943                   .481 .932 .6601.284                  -17
          .3943     .2957                   .491 .820 .5831.150                  -18
     .2957          .3943                   .504 .878 .6061.217                  -19
.3943               .2957                   .499 .615 .462 .921                  -20
.2957.2957     .0986                        .462 .481 .350 .663                  -21
.2957          .3943                        .515 .719 .479 .978                  -22
.3943          .2957                        .517 .547 .383 .784                  -25
               .2957     .2957     .0986    .5441.283 .8581.825                  -01
.3943                              .2957    .6171.035 .5721.345                  -05
     .2957     .2957.0986                   .488 .762 .5331.048                  -16
```

UNCLASSIFIED

SECURITY CLASSIFICATION OF THIS PAGE (When Data Entered)

REPORT DOCUMENTATION PAGE		READ INSTRUCTIONS BEFORE COMPLETING FORM
1. REPORT NUMBER 18 AFOSR-TR- 78-1579 19	2. GOVT ACCESSION NO.	3. RECIPIENT'S CATALOG NUMBER
4. TITLE (and Subtitle) 6 STATISTICAL ANALYSIS OF STEADY STATE COMBUSTION OF COMPOSITE SOLID PROPELLANTS		5. TYPE OF REPORT & PERIOD COVERED 9 FINAL rept. 1 July 1976 - 30 Sep 78
		6. PERFORMING ORG. REPORT NUMBER 14 U-78-15
7. AUTHOR(s) 10 R. L. GLICK		8. CONTRACT OR GRANT NUMBER(s) 15 F49620-76-C-0008
9. PERFORMING ORGANIZATION NAME AND ADDRESS THIOKOL CORPORATION HUNTSVILLE DIVISION HUNTSVILLE, AL 35807		10. PROGRAM ELEMENT, PROJECT, TASK AREA & WORK UNIT NUMBERS 2308A1 61102F 16 2308
11. CONTROLLING OFFICE NAME AND ADDRESS AIR FORCE OFFICE OF SCIENTIFIC RESEARCH/NA BLDG 410 BOLLING AIR FORCE BASE, D C 20332		12. REPORT DATE 11 Nov 78 17 A1
		13. NUMBER OF PAGES 62
14. MONITORING AGENCY NAME & ADDRESS(if different from Controlling Office)		15. SECURITY CLASS. (of this report) UNCLASSIFIED
		15a. DECLASSIFICATION/DOWNGRADING SCHEDULE

16. DISTRIBUTION STATEMENT (of this Report)

12 64 p.

Approved for public release; distribution unlimited.

17. DISTRIBUTION STATEMENT (of the abstract entered in Block 20, if different from Report)

18. SUPPLEMENTARY NOTES

19. KEY WORDS (Continue on reverse side if necessary and identify by block number)

NON-STEADY BURNING
BURNING RATE ANALYSIS
OXIDIZER DECOMPOSITION
QUASI-ONE-DIMENSIONAL COMBUSTION MODEL
COMBUSTION MODEL
HETEROGENEOUS PROPELLANTS

20. ABSTRACT (Continue on reverse side if necessary and identify by block number)

A general method for extracting particle size dependent information from experimental rate/formulation data was developed from the statistical methodology. This technique was employed to correlate the data bases of Miller. Results showed that by employing an interaction parameter of 4 that both additive and additive free data could be correlated to standard error of estimate below 10.5%. The effect of steady radiant energy deposition on steady and nonsteady burning was explored.

DD FORM 1 JAN 73 1473 401 944

UNCLASSIFIED

SECURITY CLASSIFICATION OF THIS PAGE (When Data Entered)

78 11 08 052